Inorganic Chemistry
Article

Inorg. Chem. **2010**, *49*, 1615–1625 **1615**
DOI: 10.1021/ic902012z

Cationic, Neutral, and Anionic PNP Pd^{II} and Pt^{II} Complexes: Dearomatization by Deprotonation and Double-Deprotonation of Pincer Systems

Moran Feller,[†] Eyal Ben-Ari,[†] Mark A. Iron,[‡] Yael Diskin-Posner,[‡] Gregory Leitus,[‡] Linda J. W. Shimon,[‡] Leonid Konstantinovski,[‡] and David Milstein*[,†]

[†]*Department of Organic Chemistry and* [‡]*Department of Chemical Research Support, Weizmann Institute of Science, Rehovot 76100, Israel*

Received October 12, 2009

A series of cationic, neutral, and anionic Pd^{II} and Pt^{II} PNP (PNP = 2,6-bis-(di-*tert*-butylphosphinomethyl)pyridine) complexes were synthesized. The neutral, dearomatized complexes [(PNP*)MX] (PNP* = deprotonated PNP; M = Pd, Pt; X = Cl, Me) were prepared by deprotonation of the PNP methylene group of the corresponding cationic complexes [(PNP)MX][Cl] with 1 equiv of base ($KN(SiMe_3)_2$ or ^tBuOK), while the anionic complexes $[(PNP^{**})MX]^-Y^+$ (PNP** = double-deprotonated PNP; Y = Li, K) were prepared by deprotonation of the two methylene groups of the corresponding cationic complexes with either 2 equiv of $KN(SiMe_3)_2$ or an excess of MeLi. While the reaction of [(PNP)PtCl][Cl] with an excess of MeLi led only to the anionic complex without chloride substitution, reaction of [(PNP)PdCl][Cl] with an excess of MeLi led to the methylated anionic complex $[(PNP^{**})PdMe]^-Li^+$. NMR studies, X-ray structures, and density functional theory (DFT) calculations reveal that the neutral complexes have a "broken" aromatic system with alternating single and double bonds, and the deprotonated arm is bound to the ring by an exocyclic C═C double bond. The anionic complexes are best described as a π system comprising the ring carbons conjugated with the exocyclic double bonds of the deprotonated "arms". The neutral complexes are reversibly protonated to their cationic analogues by water or methanol. The thermodynamic parameters ΔH, ΔS, and ΔG for the reversible protonation of the neutral complexes by methanol were obtained.

Introduction

Late transition metal complexes of electron donating and bulky "pincer" ligands have found important applications in synthesis, bond activation, and catalysis.[1] Among these, complexes of PNP (PNP = 2,6-bis-(di-*tert*-butylphosphinomethyl)-pyridine) and PNN (PNN = 2-(di-*tert*-butylphosphinomethyl)-6-diethylaminomethyl)pyridine) ligands have recently shown diverse reactivity.[2−7] It was found that dearomatization of the pyridine core following "arm" deprotonation of the PNP and PNN complexes plays an important role in their reactivity. For example, the deprotonated [(PNN*)RuH(CO)]

*To whom correspondence should be addressed. E-mail: david.milstein@weizmann.ac.il.

(1) For recent reviews on pincer-type complexes, see: (a) Rybtchinski, B.; Milstein, D. *Angew. Chem., Int. Ed.* **1999**, *38*, 870. (b) Jensen, C. M. *Chem. Commun.* **1999**, 2443. (c) Albrecht, M.; van Koten, G. *Angew. Chem., Int. Ed.* **2001**, *40*, 3750. (d) Vigalok, A.; Milstein, D. *Acc. Chem. Res.* **2001**, *34*, 798. (e) van der Boom, M. E.; Milstein, D. *Chem. Rev.* **2003**, *103*, 1759. (f) Singleton, J. T. *Tetrahedron* **2003**, *59*, 1837. (g) Milstein, D. *Pure Appl. Chem.* **2003**, *75*, 445. (h) Rybtchinski, B.; Milstein, D. *ACS Symp. Ser.* **2004**, *885*, 70. (i) Szabo, K. J. *Synlett* **2006**, 811. (j) *The Chemistry of Pincer Compounds*; Morales-Morales, D., Jensen, C. M., Eds.; Elsevier B. V.: Oxford, 2007. (k) Benito-Garagorri, D.; Kirchner, K. *Acct. Chem. Res.* **2008**, *41*, 201.

(2) (a) Kawatsura, M.; Hartwig, J. F. *Organometallics* **2001**, *20*, 1960. (b) Stambuli, J. P.; Stauffer, S. R.; Shaughnessy, K. H.; Hartwig, J. F. *J. Am. Chem. Soc.* **2001**, *123*, 2677. (c) Gibson, D. H.; Pariya, C.; Mashuta, M. S. *Organometallics* **2004**, *23*, 2510. (d) Kloek, S. M.; Heinekey, D. M.; Goldberg, K. I. *Organometallics* **2006**, *25*, 3007. (e) Kloek, S. M.; Heinekey, D. M.; Goldberg, K. I. *Angew. Chem., Int. Ed.* **2007**, *46*, 4736. (f) Hanson, S. K.; Heinekey, D. M.; Goldberg, K. I. *Organometallics* **2008**, *27*, 1454. (g) Pelczar, E. M.; Emge, T. J.; Krogh-Jespersen, K.; Goldman, A. S. *Organometallics* **2008**, *27*, 5759. (h) van der Vlugt, J. I.; Pidko, E. A.; Vogt, D.; Lutz, M.; Spek, A. L.; Meetsma, A. *Inorg. Chem.* **2008**, *47*, 4442. (i) Tanaka, R.; Yamashita, M.; Nazaki, K. *J. Am. Chem. Soc.* **2009**, *131*, 14168.

(3) (a) Hermann, D.; Gandelman, M.; Rozenberg, H.; Shimon, L. J. W.; Milstein, D. *Organometallics* **2002**, *21*, 812. (b) Ben-Ari, E.; Gandelman, M.; Rozenberg, H.; Shimon, L. J. W.; Milstein, D. *J. Am. Chem. Soc.* **2003**, *125*, 4714. (c) Zhang, J.; Gandelman, M.; Shimon, L. J. W.; Rozenberg, H.; Milstein, D. *Organometallics* **2004**, *23*, 4026. (d) Ben-Ari, E.; Cohen, R.; Gandelman, M.; Shimon, L. J. W.; Martin, J. M. L.; Milstein, D. *Organometallics* **2006**, *25*, 3190. (e) Zhang, J.; Gandelman, M.; Herrman, D.; Leitus, G.; Shimon, L. J. W.; Ben-David, Y.; Milstein, D. *Inorg. Chim. Acta* **2006**, *359*, 1955. (f) Feller, M.; Karton, A.; Leitus, G.; Martin, J. M. L.; Milstein, D. *J. Am. Chem. Soc.* **2006**, *128*, 12400. (g) Feller, M.; Ben-Ari, E.; Gupta, T.; Shimon, L. J. W.; Leitus, G.; Diskin-Posner, Y.; Weiner, L.; Milstein, D. *Inorg. Chem.* **2007**, *46*, 10479. (h) Zhang, J.; Gandelman, M.; Shimon, L. J. W.; Milstein, D. *Dalton Trans.* **2007**, 107. (i) Zhang, J.; Gandelman, M.; Shimon, L. J. W.; Milstein, D. *Organometallics* **2008**, *27*, 3526. (j) Feller, M.; Iron, M. A.; Shimon, L. J. W.; Diskin-Posner, Y.; Leitus, G.; Milstein, D. *J. Am. Chem. Soc.* **2008**, *130*, 14374.

(4) (a) Zhang, J.; Leitus, G.; Ben-David, Y.; Milstein, D. *J. Am. Chem. Soc.* **2005**, *127*, 12429. (b) Zhang, J.; Leitus, G.; Ben-David, Y.; Milstein, D. *Angew. Chem., Int. Ed.* **2006**, *45*, 1113. (c) Gunanathan, C.; Ben-David, Y.; Milstein, D. *Science* **2007**, *317*, 790. (d) Kohl, S. W.; Weiner, L.; Schwartsburd, L.; Konstantinovski, L.; Shimon, L. J. W.; Ben-David, Y.; Iron, M. A.; Milstein, D. *Science* **2009**, *324*, 74. (e) Li, J.; Shiota, Y.; Yoshizawa, K. *J. Am. Chem. Soc.* **2009**, *131*, 13584.

Published on Web 01/12/2010

complex (PNN* = deprotonated PNN) is a highly effective catalyst in the dehydrogenative coupling of alcohols to esters,[4a] in the hydrogenation of esters to alcohols,[4b] and in the synthesis of amides from alcohols and amines with the liberation of hydrogen.[4c] This complex was also found to be active in light-driven water splitting,[4d] which also involves metal−ligand cooperation.[4e] The complex [(PNP)Ir(COE)][BF_4] (COE = cyclooctene) exhibits unusual C−H and H_2 activation via ligand−metal cooperativity, involving dearomatization−aromatization of the ligand.[5] A few other monodeprotonated PNP complexes were also reported.[7]

Recently, we reported on the dearomatized neutral (PNN*)PtCl complex that upon reaction with RLi (R = Me, Ph) gives the anionic complexes $[(PNN^*)PtClR]^-Li^+$ with decoordination of the hemilabile amine "arm".[6] Here we report that the reaction of the dearomatized neutral complexes [(PNP*)MX] (M = Pd, Pt; X = Cl, Me) with MeLi or $KN(SiMe_3)_2$ results in deprotonation of the second "arm" to give the corresponding anionic complexes $[(PNP^{**})MX]^-Y^+$ (PNP** = double deprotonated PNP; Y = Li, K). In the case of the complex [(PNP)PtCl][Cl], chloride substitution does not take place, while the complex [(PNP)PdCl][Cl] reacts with excess of MeLi to give the double-deprotonated anionic methyl complex. DFT calculations on the double-deprotonated anionic complexes reveal a π system conjugated with the exocyclic double bonds of the deprotonated "arms".

The complexes $[(PNP^{**})MX]^-Y^+$ constitute rare examples of anionic transition metal complexes lacking strong π-acceptor ligands capable of lowering the electron density at the metal center, such as CO, olefins, or electron withdrawing phosphines.[8] Deprotonation of the two benzylic "arms" of pincer complexes is also rare and, to the best of our knowledge, only two cases have been reported, involving

Scheme 1

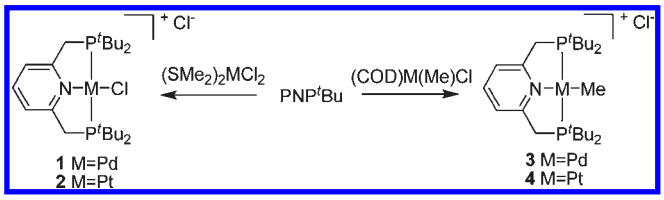

$(PNP^{Ph})Rh$ (PNP^{Ph} = (2,6-bis-(diphenylphosphinomethyl)-pyridine)[9] and (PCP)Pt (PCP = 1,3-bis(di-*tert*-butylphosphinomethyl)benzene)[10] complexes. While the anionic complexes are easily and irreversibly protonated to generate the neutral complexes by traces of water or methanol, protonation of the neutral complexes by water or methanol to form the corresponding cationic complexes is reversible.

Results and Discussion

Synthesis and Characterization of Cationic Pd^{II} and Pt^{II} Complexes. The cationic complexes [(PNP)PdCl][Cl] (**1**) and [(PNP)PtCl][Cl] (**2**) were prepared in quantitative yields by the addition of the PNP ligand to $(Me_2S)_2PdCl_2$ and $(Me_2S)_2PtCl_2$, respectively, in methylene chloride. Likewise, the cationic complexes [(PNP)PdMe][Cl] (**3**) and [(PNP)PtMe][Cl] (**4**) were prepared in quantitative yields by addition of the PNP ligand to a methylene chloride solution of (COD)Pd(Me)Cl and (COD)Pt(Me)Cl (COD = cyclooctadiene), respectively (Scheme 1). All four complexes exhibit sharp singlets in the $^{31}P\{^1H\}$ NMR spectra at 63.82, 53.69 ($^1J_{PtP}$ = 2403 Hz), 55.14 and 53.28 ($^1J_{PtP}$ = 2756 Hz) ppm for complexes **1**−**4**, respectively, indicative of two chemically equivalent phosphorus nuclei coordinated to the metal center. In the ^1H and $^{13}C\{^1H\}$ NMR spectra, the ^{t}Bu−P, CH_2−P and the pyridinic core give rise to virtual triplet signals, which also indicate equivalent phosphines. In addition, the single signal of the CH_2−P moiety in the ^1H and $^{13}C\{^1H\}$ NMR spectra is in line with C_{2v} symmetry in solution. Crystals of complexes **1**−**4** were obtained by layering pentane over methylene chloride solutions in NMR tubes. The X-ray structures of **1**−**4** (Figure 1, Table 1)[11] reveal square planar geometries with the two phosphines above and below the pyridine plane in a propeller-type geometry. The Pd−Cl, Pt−Cl, and Pd−C(1) bond lengths are shorter by 0.104,[12] 0.100,[13] and 0.135[14] Å than the analogous PCP complexes, as pyridine has a weaker *trans* influence than an aryl ring.[3d,6]

(5) (a) Ben-Ari, E.; Leitus, G.; Shimon, L. J. W.; Milstein, D. *J. Am. Chem. Soc.* **2006**, *128*, 15390. (b) Iron, M. A.; Ben-Ari, E.; Cohen, R.; Milstein, D. *Dalton Trans.* **2009**, 9433. (c) Zeng, G.; Guo, Y.; Li, S. *Inorg. Chem.* **2009**, *48*, 10257.

(6) Vuzman, D.; Povernov, E.; Shimon, L. J. W.; Diskin-Posner, Y.; Milstein, D. *Organometallics* **2008**, *27*, 2627.

(7) (a) van der Vlugt, J. I.; Lutz, M.; Pidko, E. A.; Vogt, D.; Spek, A. L. *Dalton Trans.* **2009**, *6*, 1016. (b) van der Vlugt, J. I.; Pidko, E. A.; Vogt, D.; Lutz, M.; Spek, A. L. *Inorg. Chem.* **2009**, *48*, 7513. (c) Sacco, A.; Vasapollo, G.; Nobile, C. F.; Piergiovanni, A.; Pellinghelli, M. A.; Lanfranchi, M. *J. Organometal. Chem.* **1988**, *356*, 397.

(8) (a) Benfield, F. W. S.; Forder, R. A.; Green, M. L. H.; Moser, G. A.; Prout, K. *J. Chem. Soc., Chem. Commun.* **1973**, 759. (b) Francis, B. R.; Green, M. L. H.; Tuyet, L.; Moser, G. A. *J. Chem. Soc., Dalton Trans.* **1976**, 1339. (c) Rice, G. W.; Tobias, R. S. *J. Am. Chem. Soc.* **1977**, *99*, 2141. (d) Pez, G. P.; Grey, R. A.; Corsi, J. *J. Am. Chem. Soc.* **1981**, *103*, 7528. (e) Grey, R. A.; Pez, G. P.; Wallo, A. *J. Am. Chem. Soc.* **1981**, *103*, 7536. (f) Grey, R. A.; Pez, G. P.; Wallo, A. *J. Am. Chem. Soc.* **1980**, *102*, 5948. (g) Nakazawa, H.; Ozawa, F.; Yamamoto, A. *Organometallics* **1983**, *2*, 241. (h) Bruno, J. W.; Huffman, J. C.; Green, M. A.; Caulton, K. G. *J. Am. Chem. Soc.* **1984**, *106*, 8310. (i) Del Paggio, A. A.; Andersen, R. A.; Muetterties, E. L. *Organometallics* **1987**, *6*, 1260. (j) Garcia, M. P.; Oro, L. A.; Lahoz, F. J. *Angew. Chem.* **1988**, *100*, 1766. *Angew. Chem., Int. Ed. Engl.* **1988**, *27*, 1700. (k) Brunet, J. J.; Commenges, G.; Neibecker, D.; Rosenberg, L. *J. Organomet. Chem.* **1996**, *522*, 117. (l) Gusev, D. G.; Lough, A. J.; Morris, R. H. *J. Am. Chem. Soc.* **1998**, *120*, 13138. (m) Amatore, C.; Jutand, A. *Acc. Chem. Res.* **2000**, *33*, 314. (n) Fernández, S.; Forniés, J.; Gil, B.; Gómez, J.; Lalinde, E. *Dalton Trans.* **2003**, 822. (o) Ingleson, M. J.; Pink, M.; Caulton, K. G. *J. Am. Chem. Soc.* **2006**, *128*, 4248. (p) Poverenov, E.; Gandelman, M.; Shimon, L. J. W.; Rozenberg, H.; Ben-David, Y.; Milstein, D. *Chem.—Eur. J.* **2004**, *10*, 4673. (q) Berenguer, J. R.; Lalinde, E.; Torroba, J. *Inorg. Chem.* **2007**, *46*, 9919. (r) Schwartsburd, L.; Cohen, R.; Konstantinovski, L.; Milstein, D. *Angew. Chem., Int. Ed.* **2008**, *47*, 3603.

(9) Hahn, C.; Spiegler, M.; Herdtweck, E.; Taube, R. *Eur. J. Inorg. Chem.* **1998**, 1425.

(10) Gorla, F.; Venanzi, L. M.; Albinati, A. *Organometallics* **1994**, *13*, 43.

(11) The X-ray molecular drawings of **2**−**4** and **6**−**8** are provided in the Supporting Information.

(12) Kimmich, B. F. M.; Marshall, W. J.; Fagan, P. J.; Hauptman, E.; Bullock, R. M. *Inorg. Chim. Acta* **2002**, *330*, 52.

(13) Vuzman, D.; Poverenov, E.; Diskin-Posner, Y.; Leitus, G.; Shimon, L. J. W.; Milstein, D. *Dalton Trans.* **2007**, 5692.

(14) Johansson, R.; Jarenmark, M.; Wendt, O. F. *Organometallics* **2005**, *24*, 4500.

(15) (a) Bennett, M. A.; Jin, H.; Willis, A. C. *J. Organomet. Chem.* **1993**, *451*, 249. (b) Kraatz, H. B.; Milstein, D. *J. Organomet. Chem.* **1995**, *488*, 223. (c) Dijkstra, H. P.; Meijer, M. D.; Patel, J.; Kreiter, R.; van Klink, G. P. M.; Lutz, M.; Spek, A. L.; Canty, A. J.; van Koten, G. *Organometallics* **2001**, *20*, 3159. (d) Williams, B. S.; Dani, P.; Lutz, M.; Spek, A. L.; van Koten, G. *Helv. Chim. Acta* **2001**, *84*, 3519. (e) Schwartsburd, L.; Poverenov, E.; Shimon, L. J. W.; Milstein, D. *Organometallics* **2007**, *26*, 2931. (f) Johansson, R.; Öhrström, L.; Wendt, O. F. *Cryst. Growth Des.* **2007**, *7*, 1974.

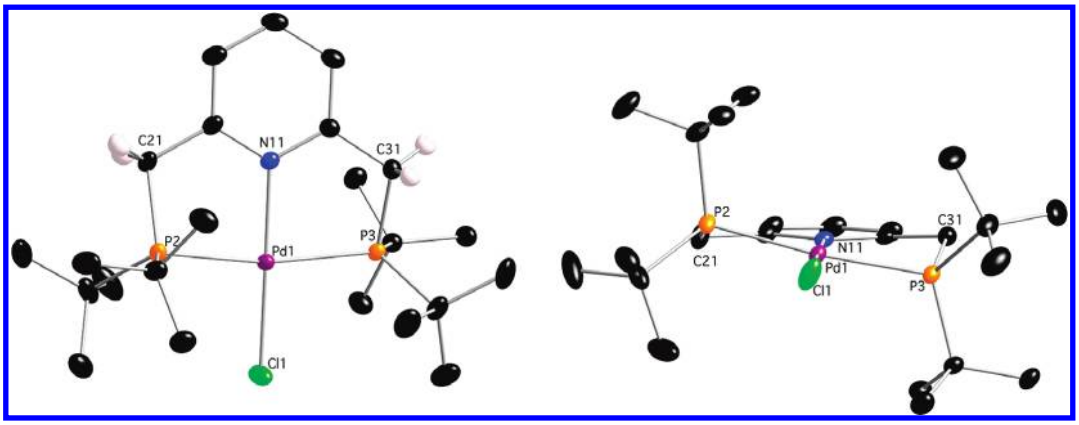

Figure 1. X-ray crystallographically determined structure of **1** showing top view (left) and side view (right) at 50% probability level. Hydrogen atoms (besides those connected to C21 and C31) and counteranions are omitted for clarity.

Table 1. Selected Bond Lengths (Å) and Bond Angles (deg) of [(PNP)PdCl][Cl] (**1**), [(PNP)PtCl][Cl] (**2**), [(PNP)PdMe][BAr_F] (**3**[$\mathbf{BAr_F}$]), [(PNP)PtMe][Cl] (**4**), [(PNP*)PdCl] (**5**), [(PNP*)PtCl] (**6**), [(PNP*)PdMe] (**7**), and [(PNP*)PtMe] (**8**)

	(**1**)[a]	(**2**)	(**3**[$\mathbf{BAr_F}$])[b]	(**4**)	(**5**)	(**6**)[c]	(**7**)[d]	(**8**)[d]
M(1)[e]−X(1)[f]	2.2927(4)	2.3066(8)	2.064(3)	2.057(2)	2.3144(12)	2.333(3)	2.067(3)	2.105(4)
M(1)−P(2)	2.2961(4)	2.3023(9)	2.3161(10)	2.2861(4)	2.3088(11)	2.312(2)	2.302(1)	2.295(1)
M(1)−P(3)	2.3010(4)	2.3030(9)	2.3186(10)	2.3006(4)	2.3039(10)	2.287(2)	2.304(1)	2.282(1)
M(1)−N(11)	2.0430(12)	2.030(3)	2.122(2)	2.1075(14)	2.038(4)	2.021(6)	2.099(2)	2.089(3)
P(2)−C(21)	1.8327(16)	1.820(3)	1.847(3)	1.836(2)	1.825(6)	1.765(8)	1.837(3)	1.754(4)
P(3)−C(31)	1.8348(16)	1.824(3)	1.851(3)	1.834(2)	1.762(5)	1.825(10)	1.764(3)	1.832(4)
C(21)−C(12)	1.498(2)	1.507(5)	1.508(5)	1.499(2)	1.491(6)	1.428(11)	1.506(4)	1.380(6)
C(31)−C(16)	1.499(2)	1.489(5)	1.509(5)	1.503(2)	1.397(6)	1.496(12)	1.382(4)	1.487(6)
P(2)−M(1)−P(3)	168.729(15)	168.32(3)	166.37(3)	164.37(2)	168.73(5)	169.22(11)	164.65(3)	164.59(4)
N(11)−M(1)−X(1)	178.44(4)	178.97(7)	179.12(14)	177.51(7)	179.43(13)	176.5(3)	178.21(11)	178.32(15)
P(2)−M(1)−N(11)	84.48(4)	83.92(8)	83.31(7)	84.07(4)	84.47(10)	84.33(17)	82.81(7)	83.58(10)
P(3)−M(1)−N(11)	84.92(4)	84.44(8)	83.15(7)	84.04(4)	84.32(10)	84.96(19)	83.99(7)	82.91(10)
P(2)−M(1)−X(1)	95.642(16)	96.36(3)	96.68(10)	96.23(6)	95.22(4)	95.69(10)	97.22(9)	96.70(11)
P(3)−M(1)−X(1)	95.055(15)	95.29(3)	96.89(10)	96.09(6)	96.00(4)	94.92(8)	96.23(9)	97.03(11)

[a] The X-ray structures of **1**, **7**, and **8** contains two molecules of the complex in the asymmetric unit cell. [b] **3**[$\mathbf{BAr_F}$] was obtained by the addition of $AgBAr_F$ to **3**. [c] The X-ray structure of **6** suggests another conformation with 13.5% occupation, which was not referred to in this table. [d] The X-ray structure of **7** and **8** contains two molecules of the complex in the asymmetric unit cell. [e] M(1) stands for Pd(1) in complexes **1**, **3**, **5**, and **7** and Pt(1) in complexes **2**, **4**, **6**, and **8**. [f] X(1) stands for Cl(1) in complexes **1**, **2**, **5**, and **6** and C(1) in complexes **3**[$\mathbf{BAr_F}$], **4**, **7**, and **8**.

The low *trans* influence of the pyridinic ring, in addition to the cationic nature of the PNP complexes **1**−**4**, has a dramatic effect on their reactivity. While the PCP analogues of the chloride complexes **1** and **2** readily react with silver salts to give the corresponding cationic complexes by abstraction of the coordinated chloride ligand,[12,14,15] complexes **1** and **2** react with $AgBF_4$, $AgPF_6$, $AgBAr^F$ (BAr^F = tetrakis-(3,5-trifluoromethylphenyl)borate), AgOTf, or $AgOC(O)CF_3$ in coordinating solvents (e.g., acetonitrile, pyridine, and tetrahydrofuran (THF)) to give only the abstraction of the outer-sphere chloride. While [(PCP)PdMe] is reactive toward CO_2 insertion,[14] complexes **3** and **4** are stable and do not react with CO_2, trityl cations, or electrophiles such as methyl iodide and methyl triflate. Surprisingly, chloride abstraction by silver salts from the less-electron rich metal center in the complex [(PNP^{Ph})PdCl][Cl] to give dicationic complexes was reported,[16] implying that inner-sphere chloride abstraction from [(PNP)PdCl][Cl] may be prevented by steric reasons.

(16) (a) Cochran, B. M.; Michael, F. E. *J. Am. Chem. Soc.* **2008**, *130*, 2786. (b) Hahn, C.; Morvillo, P.; Vitagliano, A. *Eur. J. Inorg. Chem.* **2001**, *2*, 419. (c) Hahn, C.; Vitagliano, A.; Giordano, F.; Taube, R. *Organometallics* **1998**, *17*, 2060.

Scheme 2

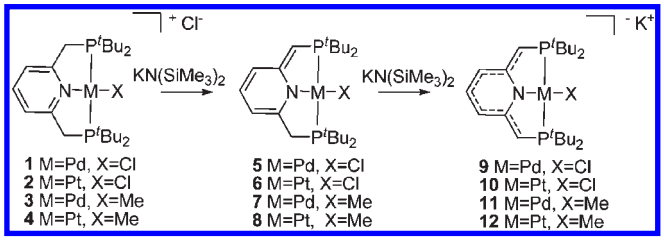

Synthesis and Characterization of Neutral Pd^{II} and Pt^{II} Complexes. The reaction of complexes **1**−**4** with 1 equiv of ^{t}BuOK or $KN(SiMe_3)_2$ in THF at ambient temperature affords the neutral, dearomatized complexes [(PNP*)PdCl] (**5**), [(PNP*)PtCl] (**6**), [(PNP*)PdMe] (**7**), and [(PNP*)PtMe] (**8**), respectively, by deprotonation of the methylene group of the "arm" (Scheme 2). Complexes **5** and **7** exhibit AB systems in the $^{31}P\{^1H\}$ NMR spectra centered at 52.22 and 61.71 ppm with $^2J_{PP}$ = 398 Hz, and at 50.67 and 53.87 ppm with $^2J_{PP}$ = 355 Hz, respectively, indicating non-equivalent phosphorus nuclei coordinated to the metal center. Complexes **6** and **8** give rise to three-spin ABX (A,B = ^{31}P, X = ^{195}Pt) systems in the $^{31}P\{^1H\}$ NMR spectra centered at

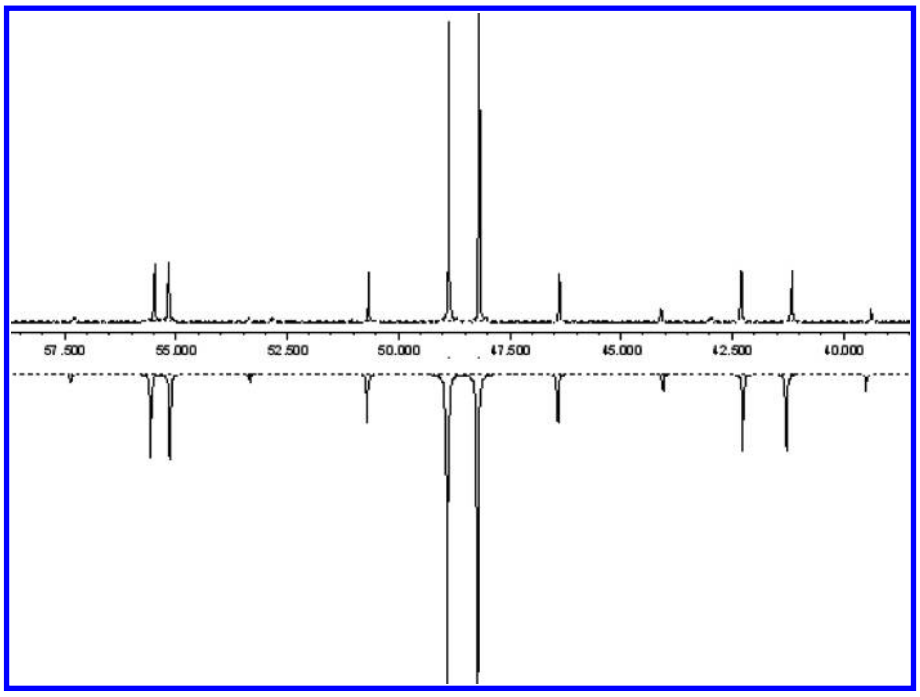

Figure 2. Experimental (above) and simulated (below) $^{31}P\{^1H\}$ NMR spectrum of [(PNP*)PtMe] (**8**) in methylene chloride-d_2 at 283 K.

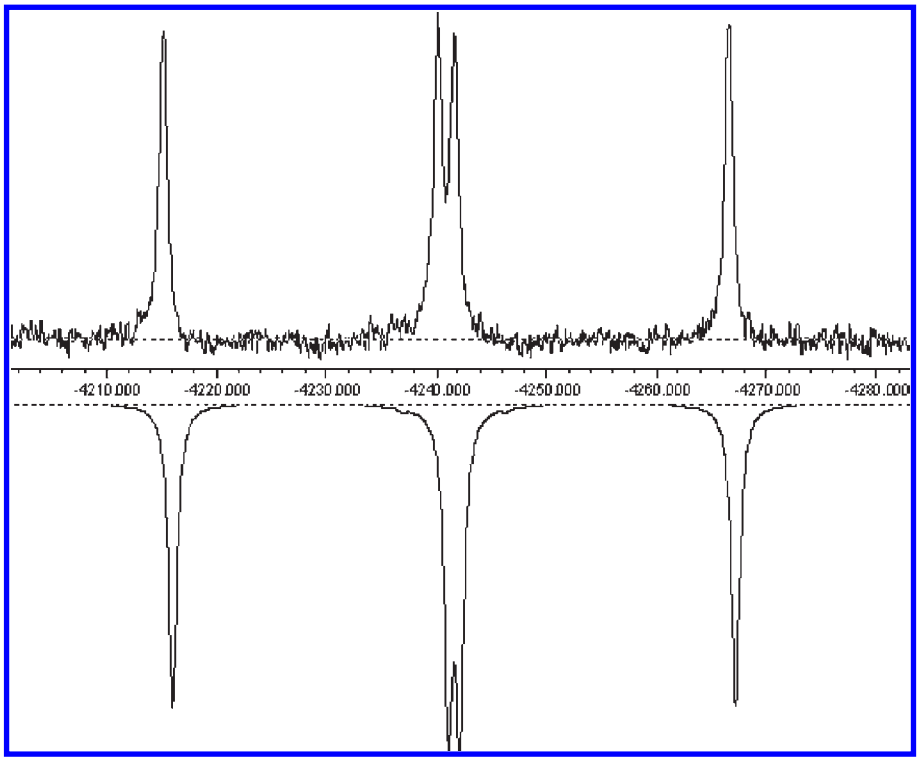

Figure 3. Experimental (above) and simulated (below) ^{195}Pt NMR spectrum of [(PNP*)PtMe] (**8**) in methylene chloride-d_2 at 283 K.

50.14 and 48.21 with $^2J_{PP}$ = 358 Hz, and at 49.76 and 47.28 with $^2J_{PP}$ = 364 Hz, respectively (Figure 2). The ^{195}Pt NMR spectrum of **8** exhibits a dd signal at −4240.4 ppm with $^1J_{PtP}$ = 2669, 2832 Hz, also indicating non-equivalent phosphorus nuclei (Figure 3). The ^{195}Pt NMR spectrum of **6** exhibits only a broad triplet signal centered at −3728 ppm.

The deprotonated "arms" of **5**−**8** give rise to a dd signal at 3.7 ppm in the ^1H NMR spectra corresponding to one proton each, and a CH dd signal at 62 (±0.1) ppm in the $^{13}C\{^1H\}$ DEPT spectra. Signals at 5.6 (±0.3), 6.4 (±0.1), and 6.6 (±0.2) ppm in the ^1H NMR of **5**−**8**, corresponding to three protons, indicate dearomatization of the pyridine ring. The dearomatized pyridine ring gives rise to five signals in the $^{13}C\{^1H\}$ NMR spectra, of which Py-C2 (which is attached to the deprotonated arm according to the HMBC spectrum) is shifted to a lower field by 11 (±0.1) ppm while Py-C4 and Py-C5 are shifted to a higher field by 10 (±0.1) ppm and Py-C3 is shifted to a higher field by 25 (±0.1) ppm in comparison to the cationic

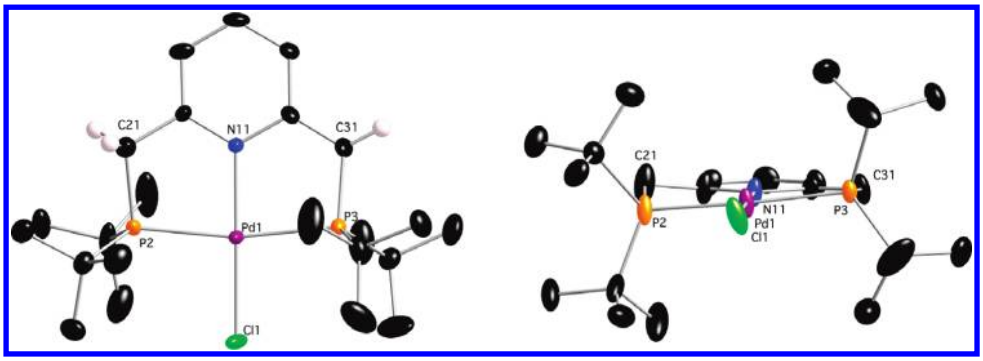

Figure 4. X-ray crystallographically determined structure of **5** at top view (left) and side view (right) at 50% probability level. Hydrogen atoms (besides those connected to C21 and C31) are omitted for clarity.

Scheme 3

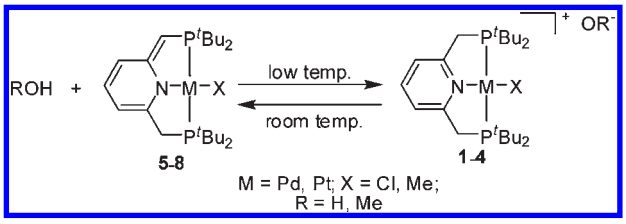

complexes **1**−**4**. The deprotonated methylene group is shifted to a lower field by 26 (±0.1) ppm while the second "arm" exhibits the same chemical shift as the methylene groups in **1**−**4**. The methyl ligands in **7** and **8** exhibit only a slight upfield shift of 1−2 ppm in the $^{13}C\{^1H\}$ NMR spectra.

Single crystal X-ray studies of **5**−**8** (Figure 4, Table 1)[11] reveal square planar geometries. The CH−C(Py) bond is shorter than the CH_2−CPy (Δ = 0.093, 0.068, 0.123, and 0.107 Å for complexes **5**−**8**, respectively), while the CH−P bond is shortened to a lesser extent than in CH_2−P bond (Δ = 0.063, 0.060, 0.072, and 0.080 Å, respectively), indicating that the non-aromatic configuration contributes much more than that of the aromatic-ylide configuration in the solid state. The five-membered ring incorporating the deprotonated arm in **5**−**8** is almost planar, with deviations of 0.0389, 0.0180, 0.0170, and 0.0298 Å, respectively, while the second five-membered ring has an envelope conformation around the CH_2 group. The M−X (M = Pd, Pt; X = Cl, Me) bonds in complexes **5**−**8** are longer than in the cationic complexes **1**−**4** (Δ = 0.022, 0.026, 0.003, and 0.048 Å, respectively), while the M−N bond lengths in the neutral complexes are slightly shorter than in their cationic analogues (Δ = 0.005, 0.009, 0.023, and 0.019 Å, respectively).

Complexes **5**−**8** undergo protonation by water or methanol to give the corresponding cationic complexes **1**−**4**. The protonation reactions are in equilibrium, as observed in the ^1H and $^{31}P\{^1H\}$ NMR spectra of the reaction mixtures.[17] At low concentrations of water or methanol, the observed signals are broad at ambient temperature (293 K), while a large excess of water or methanol shifts the equilibrium toward the cationic complexes. Variable temperature $^{31}P\{^1H\}$ NMR spectra of the reaction mixtures of **5**−**8** with excess of methanol in THF (334.7, 396.1, 44.0, and 51.4 equiv, respectively) reveal that at ambient temperature (293 K) the neutral complexes are favored while at low temperatures (213−193 K) the cationic complexes are favored (Scheme 3, Figure 5). A similar phenomenon was observed for an unsaturated (PCN)Rh^{III}Me complex, which at low temperature appears as a cationic complex while at ambient temperature the BF_4 counteranion was found to be coordinated to the metal center.[18] The cationic form is entropically disfavored because of charge separation.

As expected, the methyl complexes **7** and **8** are more basic than the chloride complexes **5** and **6**, which have a lower electron density on the metal center. The Pd complex **5** is slightly more basic than the Pt complex **6**, while the Pt complex **8** is much more basic than the Pd complex **7**. For example, addition of 335 and 396 equiv of methanol in THF to complex **5** and **6** at 193 K, respectively, resulted in 65% conversion of the neutral complexes to their cationic analogues. Addition of 44 and 51 equiv of methanol in THF at 193 K to complexes **7** and **8**, respectively, resulted in 18% and 77% conversion to the cationic complexes, respectively.

The K_{eq} for the protonation reactions with methanol described in Scheme 3 were calculated for the equilibrium reaction mixtures of **5**−**8** in THF in the temperature range of 193−223 K, in which both the cationic and neutral complexes are observed. In the case of **8**, the cationic and the neutral complexes were both only clearly observed at 193 K. The thermodynamic parameters for the protonation reaction by methanol were derived for **5**−**7** (Table 2) from the van't Hoff plots shown in Figure 6.

Synthesis and Characterization of Anionic Pd^{II} and Pt^{II} Complexes. The reaction of **5**−**8** with 1.1 equiv of $KN(SiMe_3)_2$ or of **1**−**4** with 2.1 equiv of this base afforded the rare, doubled-deprotonated anionic complexes **9**−**12** (Scheme 2). Complexes **9**−**12** were characterized in situ by NMR spectroscopy since they are not stable and react with traces of water to give the corresponding neutral complexes **5**−**8**. The $^{31}P\{^1H\}$ NMR spectra of the reaction mixtures of complexes **5**−**8** with $KN(SiMe_3)_2$ reveal sharp singlets at 55.61, 46.53 ($^1J_{PPt}$ = 2577 Hz), 50.02 and 48.77 ($^1J_{PPt}$ = 2726 Hz) ppm, respectively, indicative of two chemically equivalent phosphorus nuclei coordinated to the metal center. The ^1H NMR spectra of **9**−**12** exhibit symmetric systems, with only two signals for the pyridine moiety and one virtual triplet signal with

(17) In the case of the protonation of **5** and **6** by water, there is no clear evidence whether Cl^- or OH^- is coordinated to the metal center.

(18) Gandelman, M.; Konstantinovski, L.; Rozenberg, H.; Milstein, D. *Chem.—Eur. J.* **2003**, *9*, 2595.

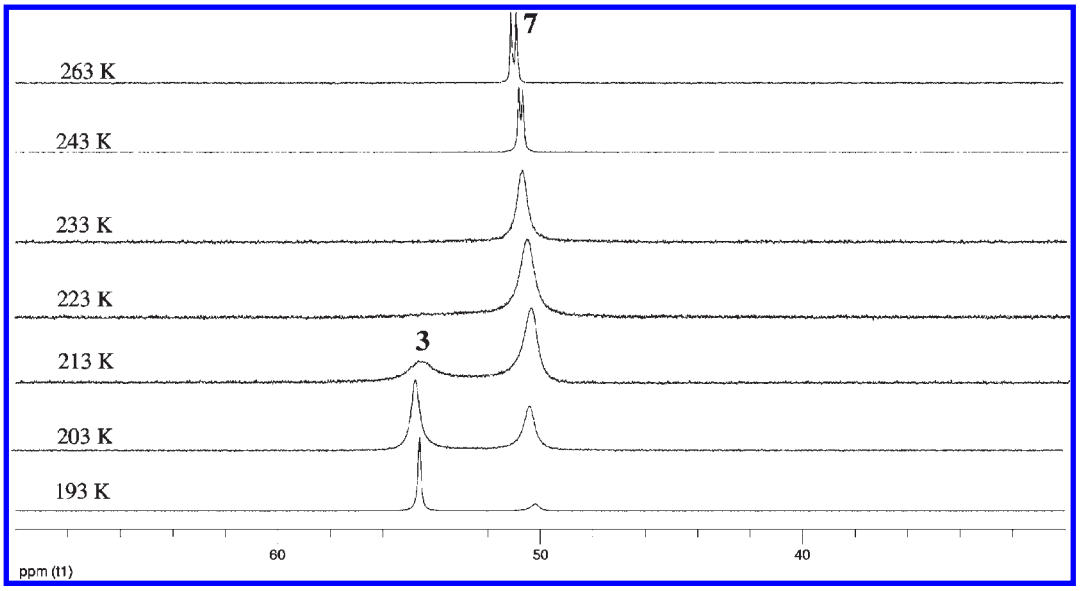

Figure 5. Variable temperature $^{31}P\{^1H\}$ (162 MHz) NMR spectrum of the reaction mixture of [(PNP*)PdMe] (**7**) (5.5 mg, 0.011 mmol) and MeOH (36.4 equiv) in THF to give [(PNP)PdMe][OMe] (**3**[**OMe**]) at low temperatures.

Table 2. Experimental Thermodynamic Parameters for the Protonation of Complexes **5**−**8** by Methanol in THF

complex	ΔH [kcal/mol]	ΔS [e.u]	ΔG^{298} [kcal/mol]	ΔG^{193} [kcal/mol]
[(PNP*)PdCl] (**5**)	−8.7 ± 1.4	−46.0 ± 6.5	5.0	0.2
[(PNP*)PtCl](**6**)	−7.0 ± 0.1	−37.8 ± 0.7	4.4	0.3
[(PNP*)PdMe] (**7**)	−11.8 ± 1.8	−54.1 ± 8.3	2.4	−2.6
[(PNP*)PtMe] (**8**)[a]				−0.5

[a] For complex **8**, the neutral and the cationic complexes were both only clearly observed at 193 K.

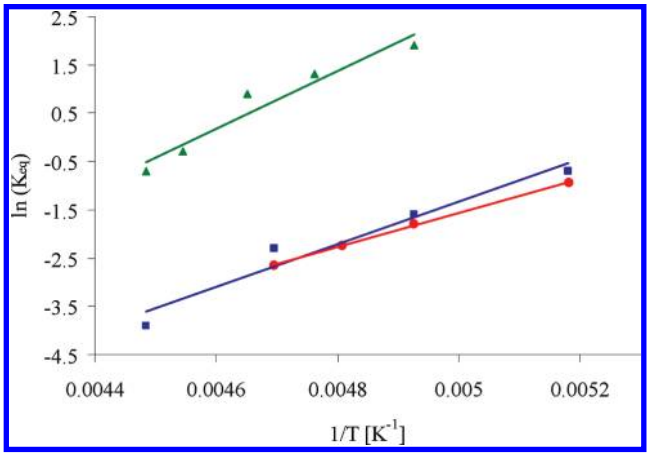

Figure 6. van't Hoff plots for the protonation by methanol in THF of complexes **5** (blue squares, 334.7 equiv of MeOH, R^2 = 0.9529), **6** (red circles, 396.1 equiv of MeOH, R^2 = 0.9991) and **7** (green triangles, 42.6 equiv of MeOH, R^2 = 0.9359).

an integration of two protons for the benzylic arms. The $^{13}C\{^1H\}$ NMR spectra of **9**−**12** exhibit a virtual triplet signal for the deprotonated benzylic arms at 50 (±1) ppm, which is assigned as CH−P by $^{13}C\{^1H\}$ DEPT, again indicative of two equivalent phosphines. The pyridine ring results in only three signals, of which Py-C2,6 and Py-C3,4 are virtual triplets. The chemical shifts of Py-C2,6 are shifted to a lower field by 12 ppm in comparison to

Scheme 4

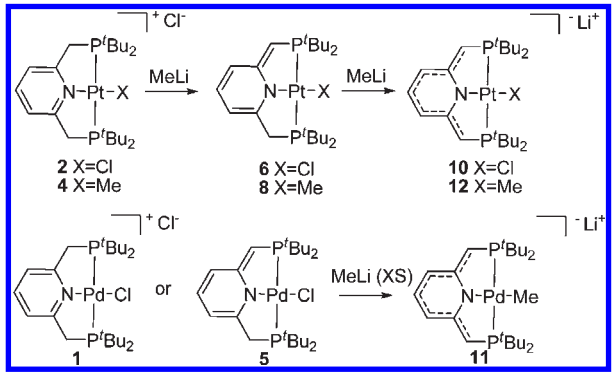

Table 3. Calculated Bond Lengths (Å) and Wiberg Bond Indices for **1′**, **5′**, and **9′**

	[(PNP)PdCl]$^+$ (**1′**)		[(PNP*)PdCl] (**5′**)		[(PNP**)PdCl]$^-$ (**9′**)	
bond[a]	bond length	Wiberg	bond length	Wiberg	bond length	Wiberg
1	1.374	1.28	1.408	1.13	1.401	1.16
2	1.374	1.28	1.378	1.24	1.401	1.16
3	1.399	1.42	1.443	1.18	1.428	1.25
4	1.399	1.42	1.384	1.50	1.428	1.25
5	1.398	1.43	1.374	1.62	1.396	1.44
6	1.398	1.43	1.424	1.27	1.396	1.44
7	1.511	1.04	1.396	1.49	1.418	1.38
8	1.511	1.04	1.512	1.03	1.418	1.38
9	1.865	0.90	1.768	1.02	1.752	1.08
10	1.865	0.90	1.855	0.91	1.752	1.08
11	2.309	0.42	2.305	0.47	2.318	0.42
12	2.068	0.42	2.324	0.38	2.318	0.42
13	2.068	0.29	2.056	0.34	2.050	0.39
14	2.348	0.48	2.381	0.42	2.421	0.37

[a] See Chart 1 for bond numbering scheme.

the cationic complexes **1**−**4**, while Py-C3,5 and Py-C4 are shifted to a higher field by 33 and 7 ppm, respectively. The deprotonated methylene group is shifted to a lower field by 15 ppm. The methyl ligands in complexes **11** and **12**

Table 4. APT Charges for Complexes **1′**−**12′**

atom	**1′**	**2′**	**3′**	**4′**	**5′**	**6′**	**7′**	**8′**	**9′**	**10′**	**11′**	**12′**
1	0.192	0.209	0.206	0.228	0.597	0.598	0.637	0.655	0.805	0.801	0.836	0.848
2	0.192	0.209	0.209	0.226	0.373	0.377	0.396	0.405	0.805	0.801	0.836	0.847
3	−0.163	−0.169	−0.171	−0.179	−0.287	−0.296	−0.317	−0.331	−0.634	−0.629	−0.639	−0.647
4	−0.163	−0.169	−0.168	−0.181	−0.463	−0.458	−0.487	−0.492	−0.634	−0.629	−0.641	−0.647
5	0.149	0.160	0.143	0.157	0.310	0.314	0.321	0.332	0.569	0.564	0.545	0.554
6	−0.138	−0.200	−0.275	−0.333	−0.415	−0.417	−0.518	−0.540	−0.492	−0.474	−0.605	−0.612
7	−0.251	−0.261	−0.231	−0.229	−0.859	−0.879	−0.884	−0.897	−0.948	−0.957	−0.949	−0.955
8	−0.251	−0.261	−0.227	−0.232	−0.191	−0.194	−0.170	−0.165	−0.948	−0.957	−0.948	−0.954
9	−0.003	0.134	−0.214	−0.064	0.003	0.112	−0.202	−0.073	−0.017	0.082	−0.201	−0.075
10	1.051	1.022	1.048	0.981	1.229	1.229	1.249	1.214	1.211	1.189	1.247	1.202
11	1.051	1.022	1.052	0.974	1.020	0.959	1.030	0.948	1.211	1.189	1.240	1.193
12	−0.426	−0.396	0.107	0.155	−0.500	−0.490	0.060	0.076	−0.553	−0.546	0.040	0.062

exhibit only slight upfield shifts of 3−4 ppm in the $^{13}C\{^1H\}$ NMR spectra.

Complexes **10** and **12** can be obtained by the reaction of **2** and **4** with 2.1 equiv of MeLi or from **6** and **8** with 1.1 equiv of MeLi. Chloride substitution does not occur even with excess of MeLi (Scheme 4).[19] However, the reaction of [(PNP)PdCl][Cl] (**1**) or [(PNP*)PdCl] (**5**) complexes with an excess of MeLi (10−20 equiv) affords the double-depronated methyl complex [(PNP**)PdMe][Li] (**11**). The reactions of **1** with 2 equiv of MeLi or of **5** with 1 equiv of MeLi are not selective. Substitution of a chloride ligand by MeLi and PhLi was reported for the neutral complexes (PNP′Bu)NiCl[7b] and (PNN)PtCl.[6]

DFT Calculations. The NMR measurements of **9**−**12** indicate symmetric complexes, implying aromatic systems in which the negative charges are localized on the two "arms", including the possibility of an ylide-type (i.e., C═P) configuration. On the other hand the ^{13}C NMR chemical shifts of **9**−**12** imply dearomatization, which can exist only in an asymmetric complex. To clarify the structure of **9**−**12**, DFT calculations were carried out on model complexes where the *tert*-butyl substituents on the phosphines were replaced by methyl groups. The bond lengths, Wiberg bond indices, and partial atomic (APT, atomic polar tensor) charges were calculated for the analogue complexes of **1**−**12** (i.e., **1′**−**12′**) (Tables 3 and 4, Chart 1, and in the Supporting Information, Tables S1−S3).

The structures of the calculated complexes **1′**−**4′** and **5′**−**8′** are similar to the "real" complexes and are in line with their X-ray structures (Table 1). The cationic complexes **1′**−**4′** have an aromatic ring with bond lengths in the 1.37−1.40 Å range and Wiberg bond indices of about 1.4, while the bonds to the "arms" are clearly single bonds (1.51 Å, bond indices of 1.0). The neutral complexes **5′**−**8′** exhibit a "broken" aromatic system with alternating single and double bonds. The deprotonated "arm" is connected to the ring by a double bond. The bond lengths and indices are indicative of a delocalized bond system like in hexatriene.

The calculted double-deprotonated complexes **9′**−**12′** can be described as bearing a π-system comprising the ring carbons and the exocyclic double bonds (Scheme 5). The bonds involved are intermediate, in both bond length and index, between single and double bonds. The two

Scheme 5

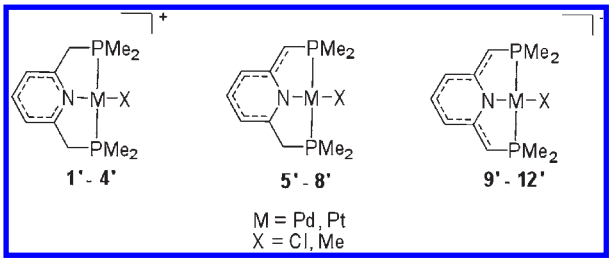

Chart 1. Numbering of Bonds (left) and Atoms (right) for Complexes **1′**−**12′** in Tables 3, 4 and Supporting Information,Tables S1−S3 (M = Pd, Pt; X = Cl, Me)

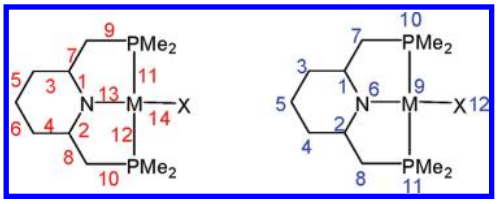

C−N bonds have more of a single bond nature (1.40 Å, bond indices of 1.2) than in the neutral complexes, and especially when compared to the cationic complexes (1.37 Å, bond indices of 1.3), showing that here the nitrogen ligand is best described as amidic rather than pyridinic, unlike the corresponding cationic complexes (Scheme 5).

All the complexes (**1′**−**12′**, Chart 1) have planar ring systems. In addition, the arm carbons and the metal atoms are located in this same plane. In the case of the anionic complexes, it could be argued that this is an artifact of the use of symmetry during the geometry optimization. The obtained structures, however, do not have any imaginary vibrational frequencies. In addition, complex **9′** was reoptimized without any symmetry constraints, which resulted in practically identical results.

The APT charges[20] calculated for complexes **9′**−**12′** (Table 4) reveal that in going from the cationic to the neutral complexes, there is a significant negative charge accumulation on one of the benzylic arms. In going to the anionic complexes, the second arm also accumulates negative charge. In all cases, the negative charge is nearly one unit of charge. Part of this charge is offset by accumulation of positive charge in the ring. The sum of

(19) The reaction of complex **2** with a large excess of MeLi (about 50 equiv) in THF exhibits after 4 days a new signal in the $^{31}P\{^1H\}$ NMR at 72.12 ppm ($^1J_{PtP}$ = 2690 Hz) (20% by integration), which could not be identified. This new signal does not correspond to any of the complexes presented.

(20) In addition to the APT charges, the natural population analysis (NPA) charges were calculated; these are provided in the Supporting Information. The results and conclusions remain the same regardless of which type of charges are considered.

the charges in the ring increases on going from the cationic via the neutral to the anionic complex. For example, for the series **1′**, **5′**, and **9′**, the sum of the charges changes from 0.040 to 0.115 to 0.434. Part of the remainder of the excess negative charge on the "arm carbons" is balanced by the positive charge on the phosphorus atoms, which is not balanced by their methyl substituents.

Summary

The non-innocent PNP ligand system has a key role in the formation and reactivity of cationic, neutral, and anionic Pd^{II} and Pt^{II} complexes. The neutral and the anionic complexes are prepared by deprotonation of the "arms" of the cationic complexes with 1 or 2 equiv of base, respectively. NMR studies, X-ray crystallography, and DFT calculations reveal that the neutral complexes have a "broken" aromatic system with alternating single and double bonds, and the deprotonated arm is bound to the ring by a C=C double bond. The anionic complexes form a π-system involving the ring carbons and the exocyclic double bonds of the deprotonated "arms". The reaction of [(PNP)PtCl][Cl] (**2**) with an excess of MeLi leads only to the anionic complex [(PNP**)PtCl]Li (**10**) without chloride substitution, while reaction of [(PNP)PdCl][Cl] (**1**) with excess of MeLi leads to the methylated anionic complex [(PNP**)PdMe]Li (**9**). Whereas the anionic complexes are easily and irreversibly protonated to their neutral analogues with traces of water or methanol, the neutral complexes are reversibly protonated to their cationic analogues. The thermodynamic parameters ΔH, ΔS, and ΔG for the reversible protonation of the neutral complexes by methanol were obtained. We have demonstrated that at ambient temperature the neutral form is entropically favored, while at low temperature the cationic form is favored because of charge separation.

Experimental Section

General Procedures. All experiments with metal complexes and phosphine ligands were carried out under an atmosphere of purified nitrogen in a Vacuum Atmospheres glovebox equipped with a MO 40-2 inert gas purifier or using standard Schlenk techniques. All solvents were reagent grade or better. All nondeuterated solvents, except methylene chloride and acetone, were refluxed over sodium/benzophenone ketyl and distilled under argon atmosphere. Methylene chloride and acetone were used as received and dried over 4 Å molecular sieves and calcium sulfate, respectively.

Deuterated solvents were used as received. All the solvents were degassed with argon and kept in the glovebox over 4 Å molecular sieves (acetone was kept over calcium sulfate). Commercial $KN(SiMe_3)_2$ (95%, Fluka) was purified by dissolving in dry toluene, filtered through a short plug of Celite followed by a thorough evaporation, and used only freshly purified. Other commercially available reagents were used as received. The PNP ligand,[3a] $(Me_2S)_2PdCl_2$,[21] $(Me_2S)_2PtCl_2$,[22] (COD)PdMeCl[23] and (COD)PtMeCl[24] were prepared according to the literature procedures. ^{1}H, ^{13}C, and ^{31}P NMR spectra were recorded using a Bruker DPX-250, Bruker AMX-400 and Avance 500 NMR spectrometers. ^{195}Pt NMR spectra were recorded at 107.5 MHz using a Bruker Avance-500 NMR spectrometer. All spectra were recorded at 23 °C unless otherwise noted. ^{1}H NMR and $^{13}C\{^1H\}$ NMR chemical shifts are reported in parts per million (ppm) downfield from tetramethylsilane. In ^{1}H NMR, the chemical shifts were referenced to the residual hydrogen signal of the deuterated solvents. In $^{13}C\{^1H\}$ NMR measurements, the signals of deuterated solvents were used as a reference. ^{31}P NMR chemical shifts are reported in parts per million downfield from H_3PO_4 and referenced to an external 85% solution of phosphoric acid in D_2O. ^{195}Pt chemical shifts are reported in parts per million relative to Na_2PtCl_6 (0 ppm) and referenced to an external concentrated solution of Na_2PtCl_4 in D_2O (−1620 ppm). Abbreviations used in the description of NMR data are as follows: br, broad; s, singlet; d, doublet; t, triplet; q, quartet; m, multiplet; v, virtual. Temperature calibration of the spectrometer was performed using CH_3OH/CD_3OD. Simulated NMR spectra were done using the gNMR5 program.[34]

Computational Details. All calculations were carried out using Gaussian 03 Revision E.01[25] locally modified with the MNGFM patch;[26] this patch from the University of Minnesota adds the M06 (vide infra) family of DFT exchange-correlation functionals to the commercial version. The Minnesota06 (M06) hybrid meta-GGA DFT functional was used.[27] This functional has been shown to yield more reliable energies and reaction barrier heights for transition metal reactions than other "conventional" exchange-correlation functionals.[27,28] The basis set-RECP (relativistic effective core potential) SDD(d) was used. This is the combination of the Huzinaga−Dunning double-ζ basis set[29] on lighter elements, where the (d) denotes the use of an additional *d* polarization function on P (i.e., the D95V basis set on H, C and N; D95 on Cl and D95(d) on P), with the Stuttgart−Dresden basis set-RECP combination[30] on transition metals.

Structures were identified as minima by having zero imaginary vibrational frequencies (i.e., all eigenvalues of the Hessian were positive).

Charges reported are Atomic Polar Tensor (APT) charges.[31] Wiberg bond indices[32] and Natural Population Analysis (NPA) charges[33] were obtained from a Natural Bond Order (NBO) analysis.[33]

(21) Byers, P. K.; Canty, A. J.; Jin, H.; Kruis, D.; Markies, B. A.; Boersma, J.; van Koten, G. *Inorg. Synth.* **1998**, *32*, 162.
(22) Otto, S.; Roodt, A. *J. Organomet. Chem.* **2006**, *691*, 4626.
(23) Rülke, R. E.; Ernsting, J. M.; Spek, A. L.; Elsevier, C. J.; van Leeuwen, P. W. N. M.; Vrieze, K. *Inorg. Chem.* **1993**, *32*, 5769.
(24) Clark, H. C.; Manzer, L. E. *J. Organomet. Chem.* **1973**, *59*, 411.
(25) Frisch, M. J.; Trucks, G. W.; Schlegel, H. B.; Scuseria, G. E.; Robb, M.; Cheeseman, J. R.; Montgomery, J. A.; Vreven, J. A.; Kudin, K. N.; Burant, J. C.; Millam, J. M.; Iyengar, S. S.; Tomasi, J.; Barone, V.; Mennucci, B.; Cossi, M.; Scalmani, G.; Rega, N.; Petersson, G. A.; Nakatsuji, H.; Hada, M.; Ehara, M.; Toyota, K. ; Fukuda, R.; Hasegawa, J.; Ishida, M.; Nakajima, T.; Honda, Y.; Kitao, O.; Nakai, H.; Klene, M.; Li, X.; Knox, J. E.; Hratchian, H. P.; Cross, J. B.; Adamo, C.; Jaramillo, J; Gomperts, R.; Stratmann, R. E.; Yazyev, O.; Austin, A. J.; Cammi, R.; Pomelli, C.; Ochterski, J. W.; Ayala, P. Y.; Morokuma, K.; Voth, G. A.; Salvador, P.; Dannenberg, J. J.; Zakrzewski, V. G.; Dapprich, S.; Daniels, A. D.; Strain, M. C.; Farkas, O.; Malick, D. K.; Rabuck, A. D.; Raghavachari, K.; Foresman, J. B.; Ortiz, J. V.; Cui, Q. ; Baboul, A. G. ; Clifford, S. ; Cioslowski, J.; Stefanov, B. B.; Liu, G.; Liashenko, A.; Piskorz, P.; Komaromi, I.; Martin, R. L.; Fox, D. J.; Keith, T.; Al-Laham, M. A.; Peng, C. Y.; Nanayakkara, A.; Challacombe, M.; Gill, P. M. W.; Johnson, B.; Chen, W.; Wong, M. W.; Gonzalez, C.; Pople, J. A. *Gaussian 03*, Revision E.01; Gaussian, Inc.: Wallingford, CT, 2004.
(26) *Minnesota Gaussian Functional Module*, version 3.1; Zhao, Y.; Truhlar, D. G. with assistance from Iron, M. A.; Martin, J. M. L.; University of Minnesota: Minneapolis, MN, 2008.
(27) Zhao, Y.; Truhlar, D. G. *Theor. Chem. Acc.* **2008**, *120*, 215.
(28) Zhao, Y.; Truhlar, D. G. *Acc. Chem. Res.* **2008**, *41*, 157.
(29) Dunning Jr., T. H.; Hay, P. J. *Modern Theoretical Chemistry*; Plenum: New York, 1976; Vol. *3*, pp 1−28.
(30) Dolg, M. *Effective Core Potentials. In Modern Methods and Algorithms of Quantum Chemistry*; John von Neumann Institute for Computing: Jülich, 2000; Vol. *1*, pp 479−508.
(31) Cioslowski, J. *J. Am. Chem. Soc.* **1989**, *111*, 8333.
(32) Wiberg, K. B. *Tetrahedron* **1968**, *24*, 1083.
(33) Reed, A. E.; Curtiss, L. A.; Weinhold, F. *Chem. Rev.* **1988**, *88*, 899.
(34) Budzelaar, P. H. M. NMR simiulation program gNMR, Version 5.0.6.0 IvorySoft, 2006.

[(PNP)PdCl][Cl] (1). A methylene chloride solution (5 mL) of PNP (150 mg, 0.379 mmol) was added to a methylene chloride solution (5 mL) of $(Me_2S)_2PdCl_2$ (114.3 mg, 0.379 mmol), and the reaction mixture was stirred for 10 min. The solvent was removed under vacuum to give a light yellow solid, which was washed with pentane (3 × 5 mL) and dried under vacuum to give complex **1** in quantitative yield. Crystals suitable for X-ray analysis were obtained by layering a concentrated methylene chloride solution of **1** with pentane.

$^{31}P\{^1H\}$ NMR (162 MHz, DCM-d_2): 63.82 (s). ^1H NMR (400 MHz, DCM-d_2): 1.45 (vt, 36H, J_{PH} = 8.0 Hz, C(CH_3)$_3$)), 4.06 (vt, 4H, J_{PH} = 3.3 Hz, CH_2-P), 7.94−8.00 (m, 3H, PNP-aryl H). $^{13}C\{^1H\}$ NMR (101 MHz, DCM-d_2): 28.86 (vt, J_{CP} = 2.4 Hz, C(CH_3)$_3$)), 35.97 (vt, J_{CP} = 9.1 Hz, CH_2-P), 36.81 (vt, J_{CP} = 8.4 Hz, C(CH$_3$)$_3$)), 123.72 (vt, J_{CP} = 5.5 Hz, PNP aryl-CH), 141.35 (s, PNP aryl-CH), 165.23 (vt, J_{CP} = 4.1 Hz, PNP aryl-C). Anal. For $C_{23}H_{43}NP_2PdCl_2$: Calcd: C, 48.22; H, 7.57; Found: C, 47.42; H, 7.66.

X-ray Structural Analysis of 1. Crystal Data. 2($C_{23}H_{43}ClNP_2$-Pd) + 2CH_2Cl_2 + H_2O + 2Cl, yellow chunk, 0.25 × 0.25 × 0.10 mm^3, triclinic, $P\bar{1}$, a = 11.2479(7) Å, b = 16.8435(11) Å, c = 17.2519(11) Å, α = 77.101(3)°, β = 78.669(3)°, γ = 87.601(3)° from 27 degrees of data, T = 100(2) K, V = 3123.9(3) Å^3, Z = 2, fw = 1333.52, Dc = 1.418 Mg/m^{-3}, μ = 1.054 mm^{-1}.

Data Collection and Processing. Bruker APEX-II KappaCCD diffractometer, Mo Kα (λ = 0.71073 Å), graphite monochromator, $-16 \le h \le 14$, $-24 \le k \le 10$, $-24 \le l \le 24$, frame scan width = 0.5°, scan speed 1.0° per 16 s, typical peak mosaicity 0.77°, 65960 reflections collected, 19259 independent reflections (R_{int} = 0.0268). The data were processed with APEXII.

Solution and Refinement. Structure solved by direct methods with Bruker Autostructure. Full matrix least-squares refinement based on F^2 and empirical absorption correction with SHELXL-97; 612 parameters with no restraints, final R_1 = 0.0240 (based on F^2) for data with I > 2σ(I), R_1 = 0.0330 on 19241 reflections, goodness-of-fit on F^2 = 1.076, largest electron density peak = 0.505 e Å^{-3}.

[(PNP)PtCl][Cl] (2). Complex **2** was synthesized in the same manner as complex **1** from $(Me_2S)_2PtCl_2$ (56.3 mg, 0.144 mmol) and PNP (56.9 mg, 0.144 mmol), and was obtained in quantitative yield as a yellow solid. Crystals suitable for X-ray analysis were obtained by layering a concentrated methylene chloride solution of **2** with pentane.

$^{31}P\{^1H\}$ NMR (101 MHz, DCM-d_2): 53.69 (s, $^1J_{PPt}$ = 2403 Hz). ^1H NMR (250 MHz, DCM-d_2): 1.41 (vt, 36H, J_{PH} = 7.5 Hz, C(CH_3)$_3$), 3.98 (vt, 4H, J_{PH} = 3.7 Hz, CH_2-P), 7.7−8.3 (m, 3H, PNP-aryl H). $^{13}C\{^1H\}$ NMR (63 MHz, DCM-d_2): 28.71 (vt, J_{CP} = 2.2 Hz, C(CH_3)$_3$), 36.01 (vt, J_{CP} = 12.5 Hz, CH_2-P), 36.57 (vt, J_{CP} = 12.5 Hz, C(CH$_3$)$_3$), 123.58 (vt, J_{CP} = 5.1 Hz, PNP aryl-CH), 140.43 (s, PNP aryl-CH), 165.32 (vt, J_{CP} = 3.6 Hz, PNP aryl-C). Anal. For $C_{23}H_{44}Cl_2NP_2Pt$: Calcd: C, 41.76; H, 6.55; Found: C, 41.56; H, 6.62.

X-ray Structural Analysis of 2. Crystal Data. $C_{23}H_{43}$-$ClNP_2Pt$+Cl, colorless, needle, 0.20 × 0.06 × 0.06 mm^3, hexagonal, $P\bar{3}$, a = b = 18.631(3) Å, c = 14.821(2) Å, from 10924 reflections, T = 120(2) K, V = 4455.3(13) Å^3, Z = 6, fw = 661.51, Dc = 1.479 Mg/m^{-3}, μ = 5.021 mm^{-1}.

Data Collection and Processing. Nonius KappaCCD diffractometer, Mo Kα (λ = 0.71073 Å), graphite monochromator, $-28 \le h \le 14$, $0 \le k \le 28$, $0 \le l \le 22$, frame scan width = 1.0°, scan speed 1.0° per 60 s, typical peak mosaicity 0.54°, 11284 independent reflections collected, (R_{int} = 0.066). The data were processed with Denzo-Scalepack.

Solution and Refinement. Structure solved by direct methods with SHELXS-97. Full matrix least-squares refinement based on F^2 and empirical absorption correction with SHELXL-97; 274 parameters with 0 restraints, final R_1 = 0.0387 (based on F^2) for data with I > 2σ(I), and R_1 = 0.0603 on 11284 reflections, goodness-of-fit on F^2 = 1.014, largest electron density peak = 3.971 e Å^{-3} and hole = −1.392 e Å^{-3}.

[(PNP)PdMe][Cl] (3). A methylene chloride solution (5 mL) of PNP (149.0 mg, 0.377 mmol) was added to a methylene chloride solution (5 mL) of (COD)PdMeCl (100 mg, 0.377 mmol) to give a colorless solution, and the reaction mixture was stirred for 10 min. The solvent was removed under vacuum to give a white solid, which was washed with pentane (3 × 5 mL) and dried under vacuum, to give complex **3** in quantitative yield. [(PNP)-PdMe][BAr_F] (**3**[**BAr$_F$**]) was obtained by addition of $AgBAr_F$ (87.3 mg, 0.09 mmol) to a methylene chloride solution (5 mL) of **3** (50 mg, 0.09 mmol). The reaction mixture was stirred at dark for an hour, followed by filtration over Celite. The solvent was removed by vacuum to give **3**[**BAr$_F$**] in quantitative yield. Crystals suitable for X-ray analysis were obtained by slow evaporation of methylene chloride solution of **3**[**BAr$_F$**]. Crystals of **3** were obtained by layering a concentrated methylene chloride solution of **3** with pentane.

$^{31}P\{^1H\}$ NMR (162 MHz, DCM-d_2): 55.14 (s). ^1H NMR (400 MHz, DCM-d_2): 0.62 (t, 3H, $^3J_{PH}$ = 5.4 Hz, Pd-CH_3), 1.14 (vt, 36H, J_{PH} = 7.2 Hz, C(CH_3)$_3$)), 3.61 (vt, 4H, J_{PH} = 3.7 Hz, CH_2-P), 7.48 (d, 2H, $^3J_{HH}$ = 7.8 Hz, PNP-aryl H), 7.71 (t, 1H, $^3J_{HH}$ = 7.8 Hz, PNP-aryl H). $^{13}C\{^1H\}$ NMR (101 MHz, DCM-d_2): −16.27 (t, $^2J_{CP}$ = 4.3 Hz, Pd-CH_3), 29.18 (vt, J_{CP} = 3.0 Hz, C(CH_3)$_3$)), 35.67 (vt, J_{CP} = 7.8 Hz, C(CH$_3$)$_3$)), 36.89 (vt, J_{CP} = 9.1 Hz, CH_2-P), 122.41 (vt, J_{CP} = 4.5 Hz, PNP aryl-CH), 140.39 (s, PNP aryl-CH), 161.20 (vt, J_{CP} = 4.1 Hz, PNP aryl-C). Anal. For $C_{24}H_{46}NP_2PdCl$: Calcd: C, 52.18; H, 8.39; Found: C, 53.32; H, 8.72.

X-ray Structural Analysis of 3. Crystal Data. $C_{24}H_{46}NP_2Pd$ + $C_{32}H_{12}BF_{24}$ + $C_4H_{10}O$, orange, prism, 0.2 × 0.3 × 0.3 mm^3, monoclinic, $P2_{1/c}$, a = 13.583(3) Å, b = 24.177(5) Å, c = 20.219(4) Å, β = 98.40(3)°, from 27 degrees of data, T = 120(2) K, V = 6569(2) Å^3, Z = 4, fw = 1454.30, Dc = 1.471 Mg/m^{-3}, μ = 0.439 mm^{-1}.

Data Collection and Processing. Nonius KappaCCD diffractometer, Mo Kα (λ = 0.71073 Å), graphite monochromator, $0 \le h \le 17$, $0 \le k \le 31$, $-26 \le l \le 25$, frame scan width = 1.0°, scan speed 1.0° per 60 s, typical peak mosaicity 0.4410°, 15162 independent reflections collected, (R_{int} = 0.055). The data were processed with Denzo-Scalepack.

Solution and Refinement. Structure solved by direct methods with SHELXS-97. Full matrix least-squares refinement based on F^2 and empirical absorption correction with SHELXL-97; 881 parameters with 0 restraints, final R_1 = 0.0532 (based on F^2) for data with I > 2σ(I), and R_1 = 0.0886 on 14783 reflections, goodness-of-fit on F^2 = 1.051, largest electron density peak = 0.792 e Å^{-3} and hole = −0.765 e Å^{-3}.

[(PNP)PtMe][Cl] (4). Complex **4** was synthesized in the same manner as complex **3** from PNP (100.0 mg, 0.253 mmol) and (COD)PtMeCl (89.5 mg, 0.253 mmol), and was obtained in quantitative yield as a white solid. Crystals suitable for X-ray analysis were obtained by layering a concentrated methylene chloride solution of **4** with pentane.

$^{31}P\{^1H\}$ NMR (101 MHz, DCM-d_2): 53.28 (s, $^1J_{PPt}$ = 2756 Hz). ^1H NMR (500 MHz, DCM-d_2): 1.21 (t, 3H, $^3J_{PH}$ = 3.2 Hz, Pt-CH_3), 1.35 (vt, 36H, J_{PH} = 7.2 Hz, C(CH_3)$_3$), 3.70 (vt, 4H, J_{PH} = 3.7 Hz, CH_2-P), 7.61 (d, 2H, $^3J_{HH}$ = 8.1 Hz, PNP-aryl H), 7.96 (t, 1H, $^3J_{HH}$ = 8.1 Hz, PNP-aryl H). $^{13}C\{^1H\}$ NMR (126 MHz, DCM-d_2): −28.45 (t, $^2J_{CP}$ = 6.3, $^1J_{CPt}$ = 623.5 Hz, Pt-CH_3), 28.90 (vt, J_{CP} = 2.5 Hz, C(CH_3)$_3$), 36.10 (vt, J_{CP} = 11.3 Hz, CH_2-P), 37.57 (vt, J_{CP} = 12.6 Hz, C(CH$_3$)$_3$), 122.16 (vt, J_{CP} = 4.4 Hz, PNP aryl-CH), 139.64 (s, PNP aryl-CH), 161.99 (vt, J_{CP} = 3.1 Hz, PNP aryl-C). Anal. For $C_{24}H_{46}NP_2PtCl$: Calcd: C, 44.96; H, 7.23; Found: C, 44.28; H, 7.48.

X-ray Structural Analysis of 4. Crystal Data. $C_{24}H_{46}NP_2Pt$ + Cl^- + $CHCl_3$, colorless prism, 0.50 × 0.12 × 0.12 mm^3, triclinic, $P\bar{1}$, a = 14.5689(8) Å, b = 15.4434(4) Å, c = 16.2371(5) Å, α = 114.733(1)°, β = 99.124(2)°, γ = 96.400(2)° from 89865 reflections, T = 100(2) K, V = 3211.1(2) Å^3, Z = 4, fw = 760.47, Dc = 1.573 Mg/m^{-3}, μ = 4.817 mm^{-1}.

Data Collection and Processing. Bruker KappaAPEX-II diffractometer, Mo Kα (λ = 0.71073 Å), graphite monochromator, $-22 \le h \le 22$, $-23 \le k \le 23$, $-25 \le l \le 25$, frame scan width = 0.5°, scan speed 1.0° per 10 s, typical peak mosaicity 0.69°, 89840 reflections collected, 24730 independent reflections (R_{int} = 0.0403). The data were processed with APEX II.

Solution and Refinement. Structure solved by Bruker AutoStructure. Full matrix least-squares refinement based on F^2 and empirical absorption correction with SHELXL-97; 622 parameters with no restraints, final R_1 = 0.0205 (based on F^2) for data with I > 2σ(I), R_1 = 0.0257 on 24725 reflections, goodness-of-fit on F^2 = 0.849, largest electron density peak = 2.558 e Å^{-3}. Largest hole −1.863 e Å^{-3}.

[(PNP*)PdCl] (5). To a suspension of [(PNP)PdCl][Cl] (**1**) (66.7 mg, 0.116 mmol) in THF (5 mL), was added ^{t}BuOK (14.0 mg, 0.125 mmol) or KN(SiMe$_3$)$_2$ (24.9 mg, 0.125 mmol), and the reaction mixture turned to a clear brown solution. The solution was stirred at ambient temperature for 30 min, and the solvent was removed under vacuum. The residue was extracted with benzene. The extracts were combined and filtered through a cotton pad and Celite, and the solvent was removed under vacuum, resulting in complex **5** as a brown powder in 87% (54.2 mg) yield. Crystals suitable for X-ray analysis were obtained by slow evaporation of benzene solution of **5**.

^{31}P{^{1}H} NMR (202 MHz, THF-d_8): AB system centered at 52.22 and 61.71 (d, $^2J_{PP}$ = 397.9 Hz). ^{1}H NMR (400 MHz, THF-d_8): 1.61 (vt, 36H, J_{PH} = 12.0, C(CH_3)$_3$)), 3.31 (vt, 2H, J_{PH} = 10.0 Hz, CH_2-P), 3.78 (br s, 1H, *CH*-P), 5.60 (d, 1H, $^3J_{HH}$ = 6.6 Hz, PNP-aryl H), 6.25 (d, 1H,$^3J_{HH}$ = 9.0 Hz, PNP-aryl H), 6.5 (m, 1H, PNP-aryl H). ^{13}C{^{1}H} NMR (126 MHz, THF-d_8): 29.08 (dd, $^2J_{CP}$ = 3.7, $^4J_{CP}$ = 1.8 Hz, C(CH_3)$_3$)), 29.47 (dd, $^2J_{CP}$ = 3.7, $^4J_{CP}$ = 1.8 Hz, C(CH_3)$_3$)), 34.46 (dd, $^1J_{CP}$ = 19.4, $^3J_{CP}$ = 2.8 Hz, CH_2-P), 35.86 (dd, $^1J_{CP}$ = 10.5, $^3J_{CP}$ = 3.7 Hz, *C*(CH$_3$)$_3$)), 38.00 (dd, $^1J_{CP}$ = 20.3, $^3J_{CP}$ = 4.6 Hz, *C*(CH$_3$)$_3$)), 61.49 (dd, $^1J_{CP}$ = 54.6, $^3J_{CP}$ = 1.8 Hz, *CH*-P), 99.00 (d, $^3J_{CP}$ = 12.9 Hz, PNP aryl-CH), 114.19 (d, $^3J_{CP}$ = 19.4 Hz, PNP aryl-CH), 132.63 (s, PNP aryl-CH), 160.90 (dd, $^2J_{CP}$ = 7.4, $^4J_{CP}$ = 1.8 Hz, PNP aryl-C), 173.48 (dd, $^2J_{CP}$ = 18.5, $^4J_{CP}$ = 2.8 Hz, PNP aryl-C). Anal. For $C_{23}H_{43}NP_2PdCl$: Calcd: C, 51.40; H, 8.06; Found: C, 52.09; H, 7.96.

X-ray Structural Analysis of 5. Crystal Data. $C_{23}H_{42}ClNP_2Pd$, dark red chunk, 0.30 × 0.30 × 0.05 mm^3, orthorhombic, *Pna*2$_1$, a = 22.4434(14) Å, b = 8.0692(6) Å, c = 14.1822(11)Å, from 16885 reflections, T = 100(2) K, V = 2568.4(3) Å^3, Z = 4, fw = 536.37, Dc = 1.387 Mg/m^{-3}, μ = 0.961 mm^{-1}.

Data Collection and Processing. Bruker KappaApex-II CCD diffractometer, Mo Kα (λ = 0.71073 Å), graphite monochromator, $-32 \le h \le 31$, $-11 \le k \le 10$, $-9 \le l \le 20$, frame scan width = 0.5°, scan speed 1.0° per 20 s, typical peak mosaicity 0.73°, 15985 reflections collected, 5254 independent reflections (R_{int} = 0.0197). The data were processed with APEX2.

Solution and Refinement. Structure solved by direct methods with Bruker AutoStructure. Full matrix least-squares refinement based on F^2 and empirical absorption correction with SHELXL-97; 266 parameters with one restraints, final R_1 = 0.0401 (based on F^2) for data with I > 2σ(I), and R_1 = 0.0422 on 5254 reflections, goodness-of-fit on F^2 = 1.088, largest electron density peak = 3.331 e Å^{-3}. Largest hole −2.219 e Å^{-3}.

[(PNP*)PtCl] (6). Complex **6** was synthesized in the same manner as complex **5** from [(PNP)PtCl][Cl] (**2**) (70.0 mg, 0.106 mmol). **6** was obtained as a yellow solid in quantitative yield. Crystals suitable for X-ray analysis were obtained by slow evaporation of benzene solution of **6**.

^{31}P{^{1}H} NMR (101 MHz, benzene-d_6): AB system centered at 50.14 and 48.21 ($^2J_{PP}$ = 358 Hz). ^{195}Pt NMR (107 MHz, benzene-d_6): −3728 (br s). ^{1}H NMR (250 MHz, benzene-d_6): 1.18 (m, 18H, C(CH_3)$_3$), 1.52 (m, 18H, C(CH_3)$_3$), 2.50 (m, 2H, CH_2-P), 3.71 (vt, 1H, J_{PH} = 4.5 Hz, $^3J_{PtH}$ = 15 Hz, *CH*-P), 5.35 (d, 1H, $^3J_{HH}$ = 6.5 Hz, PNP-aryl H), 6.45−6.30 (m, 2H, PNP-aryl H). ^{13}C{^{1}H} NMR (63 MHz, benzene-d_6): 28.62 (br s, C(CH_3)$_3$), 29.35 (vt, J_{CP} = 2.5 Hz, C(CH_3)$_3$), 34.65 (dd, $^3J_{CP}$ = 4.6 Hz, $^1J_{CP}$ = 18.0 Hz, CH_2-P), 35.15 (dd, $^3J_{CP}$ = 7.5 Hz, $^1J_{CP}$ = 14.0 Hz, *C*(CH$_3$)$_3$), 37.78 (dd, $^3J_{CP}$ = 9.8 Hz, $^1J_{CP}$ = 20.3 Hz, *C*(CH$_3$)$_3$), 63.04 (dd, $^3J_{CP}$ = 15.7 Hz, $^1J_{CP}$ = 45.4 Hz, *CH*-P), 98.03 (dd, $^4J_{CP}$ = 2.5 Hz, $^3J_{CP}$ = 8.0 Hz, PNP aryl-CH), 114.08 (dd, $^4J_{CP}$ = 4.8 Hz, $^3J_{CP}$ = 12.9 Hz, PNP aryl-CH), 131.55 (s, PNP aryl-CH), 159.35 (vt, J_{CP} = 4.2 Hz, PNP aryl-C), 173.02 (dd, $^3J_{CP}$ = 7.4 Hz, $^1J_{CP}$ = 12.0 Hz, PNP aryl-C). Anal. For $C_{23}H_{42}ClNP_2Pt$: Calcd: C, 44.19; H, 6.77; Found: C, 44.39; H, 6.88.

X-ray Structural Analysis of 6. Crystal Data. $C_{23}H_{42}ClNP_2Pt$, red plate, 0.25 × 0.10 × 0.02 mm^3, orthorhombic, *Pna*2$_1$, a = 22.4986(5) Å, b = 8.1073(2) Å, c = 14.1611(2) Å, from 25 degrees of data, T = 120(2) K, V = 2583.0(1) Å^3, Z = 4, Fw = 625.06, Dc = 1.607 Mg/m^{-3}, μ = 5.669 mm^{-1}.

Data Collection and Processing. Nonius KappaCCD diffractometer, Mo Kα (λ = 0.71073 Å), graphite monochromator, $0 \le h \le 29$, $0 \le k \le 10$, $0 \le l \le 18$, frame scan width = 1.0°, scan speed 1.0° per 30 s, typical peak mosaicity 0.546°, 26661 reflections collected, 3364 independent reflections (R_{int} = 0.075). The data were processed with Denzo-Scalepack.

Solution and Refinement. Structure solved by direct methods with SHELXS-97. Full matrix least-squares refinement based on F^2 and empirical absorption correction with SHELXL-97; 271 parameters with 7 restraints (on temperature factors of atoms C31, P3 and C16), final R_1 = 0.0307 (based on F^2) for data with I > 2σ(I), and R_1 = 0.0448 on 3066 reflections, goodness-of-fit on F^2 = 1.042, largest electron density peak = 1.514 e Å^{-3}. Largest hole −0.820 e Å^{-3}.

[(PNP*)PdMe] (7). Complex **7** was synthesized in the same manner as complex **5** from [(PNP)PdMe][Cl] (**3**) (105.0 mg, 0.190 mmol). **7** was obtained as a yellow solid in 67% yield. Crystals suitable for X-ray analysis were obtained by slow evaporation of benzene solution of **7**.

^{31}P{^{1}H} NMR (162 MHz, benzene-d_6): AB system centered at 50.67 and 53.87 (d, $^2J_{PP}$ = 355.4 Hz). ^{1}H NMR (400 MHz, benzene-d_6): 0.83 (dd ≈ t, 3H, $^3J_{PH}$ = 5.4 Hz, Pd-CH_3), 1.02 (dd, 18H, $^3J_{PH}$ = 11.2, $^5J_{PH}$ = 1.5 Hz, C(CH_3)$_3$)), 1.42 (dd, 18H, $^3J_{PH}$ = 11.7, $^5J_{PH}$ = 1.5 Hz, C(CH_3)$_3$)), 2.73 (d, 2H, $^2J_{PH}$ = 7.8 Hz, CH_2-P), 3.52 (d, 1H, $^2J_{PH}$ = 5.4 Hz, *CH*-P), 5.48 (d, 1H, $^3J_{HH}$ = 6.4 Hz, PNP-aryl H), 6.44 (d, 1H,$^3J_{HH}$ = 9.3 Hz, PNP-aryl H), 6.58 (m, 1H, PNP-aryl H). ^{13}C{^{1}H} NMR (101 MHz, benzene-d_6): −19.81 (dd ≈ t, $^2J_{CP}$ = 6.4 Hz, Pd-CH_3), 28.97 (dd, $^2J_{CP}$ = 4.6, $^4J_{CP}$ = 1.4 Hz, C(CH_3)$_3$)), 29.71 (dd, $^2J_{CP}$ = 4.8, $^4J_{CP}$ = 1.6 Hz, C(CH_3)$_3$)), 34.34 (dd, $^1J_{CP}$ = 8.7, $^3J_{CP}$ = 3.9 Hz, *C*(CH$_3$)$_3$)), 36.41 (d, $^1J_{CP}$ = 15.9 Hz, CH_2-P), 36.61 (dd, $^1J_{CP}$ = 17.2, $^3J_{CP}$ = 6.0 Hz, *C*(CH$_3$)$_3$)), 61.47 (dd, $^1J_{CP}$ = 46.9, $^3J_{CP}$ = 6.4 Hz, *CH*-P), 97.44 (d, $^3J_{CP}$ = 8.7 Hz, PNP aryl-CH), 113.12 (dd, $^3J_{CP}$ = 15.4, $^4J_{CP}$ = 2.3 Hz, PNP aryl-CH), 132.69 (s, PNP aryl-CH), 157.48 (dd, $^2J_{CP}$ = 3.2, $^4J_{CP}$ = 1.8 Hz, PNP aryl-C), 170.63 (dd, $^2J_{CP}$ = 16.0, $^4J_{CP}$ = 6.0 Hz, PNP aryl-C). Anal. For $C_{24}H_{46}NP_2Pd$: Calcd: C, 55.76; H, 8.97; Found: C, 55.73; H, 8.83.

X-ray Structural Analysis of 7. Crystal Data. $C_{24}H_{45}NP_2Pd$, orange prism, 0.1 × 0.05 × 0.05 mm^3, monoclinic, *P*2$_{1/c}$, a = 11.061(2) Å, b = 15.471(3) Å, c = 30.102(6) Å, β = 90.60(3)°, from 20 degrees of data, T = 120(2) K, V = 5150.9(18) Å^3, Z = 8, fw = 515.95, Dc = 1.331 Mg/m^{-3}, μ = 0.855 mm^{-1}.

Data Collection and Processing. Nonius KappaCCD diffractometer, Mo Kα (λ = 0.71073 Å), graphite monochromator, $0 \le h \le 14$, $0 \le k \le 20$, $-39 \le l \le 39$, frame scan width = 0.9°, scan speed 1.0° per 120 s, typical peak mosaicity 0.38°, 43218 reflections collected, 12189 independent reflections (R_{int} = 0.049). The data were processed with Denzo-Scalepack.

Solution and Refinement. Structure solved by direct methods with SHELXS-97. Full matrix least-squares refinement based on F^2 and empirical absorption correction with SHELXL-97; 553 parameters with 0 restraints, final R_1 = 0.0384 (based on F^2) for data with I > 2σ(I), and R_1 = 0.0542 on 11739 reflections, goodness-of-fit on F^2 = 1.037, largest electron density peak = 0.986 e Å^{-3}. Largest hole −0.561 e Å^{-3}.

[(PNP*)PtMe] (8). Complex **8** was synthesized in the same manner as complex **5** from [(PNP)PtMe][Cl] (**4**) (106.6 mg, 0.166 mmol). **8** was obtained as a yellow solid in quantitative yield. Crystals suitable for X-ray analysis were obtained by slow evaporation of benzene solution of **8**.

$^{31}P\{^{1}H\}$ NMR (101 MHz, DCM-d_2): AB system centered at 49.76 and 47.28 (d, $^{2}J_{PP}$ = 364 Hz). ^{195}Pt (107 MHz, DCM-d_2): 4240.4 ppm (dd, $^{1}J_{PtP}$ = 2669, 2832 Hz). ^{1}H NMR (250 MHz, benzene-d_6): 1.07 (dd, $^{5}J_{PH}$ = 4.1, $^{3}J_{PH}$ = 9.1 Hz, 18H, C(CH_3)$_3$), 1.37 (dd ≈ t, 3H, J_{PH} = 6.0 Hz, Pt-CH_3), 1.43 (dd, $^{5}J_{PH}$ = 4.1, $^{3}J_{PH}$ = 9.0 Hz, 18H, C(CH_3)$_3$), 2.71 (br d, 2H, $^{1}J_{PH}$ = 4.2 Hz, CH_2-P), 3.87 (vt, 1H, J_{PH} = 4.2, $^{3}J_{PtH}$ = 32 Hz, CH-P), 5.55 (d, 1H, $^{3}J_{HH}$ = 6.0 Hz, PNP-aryl H), 6.51−6.66 (m, 2H, PNP-aryl H). $^{13}C\{^{1}H\}$ NMR (126 MHz, THF-d_8): −30.19 (t, $^{2}J_{CP}$ = $^{2}J_{CP}$ = 7.0, $^{1}J_{CPt}$ = 615 Hz, Pt-CH_3), 28.62 (br d, $^{2}J_{CP}$ = 2.3 Hz, C(CH_3)$_3$), 29.83 (br d, J_{CP} = 2.4 Hz, C(CH_3)$_3$), 35.72 (dd, $^{3}J_{CP}$ = 5.4 Hz, $^{1}J_{CP}$ = 15.8 Hz, CH_2-P), 37.50−37.89 (m, C(CH$_3$)$_3$), 61.56 (dd, $^{3}J_{CP}$ = 6.0 Hz, $^{1}J_{CP}$ = 57.1 Hz, CH-P), 97.31 (d, $^{3}J_{CP}$ = 9.0 Hz, PNP aryl-CH), 112.61 (dd, $^{4}J_{CP}$ = 1.8 Hz, $^{3}J_{CP}$ = 14.8 Hz, PNP aryl-CH), 132.23 (s, PNP aryl-CH), 159.03 (vt, J_{CP} = 3.5, $^{2}J_{CPt}$ = 41 Hz, PNP aryl-C), 173.03 (dd, $^{3}J_{CP}$ = 5.4 Hz, $^{1}J_{CP}$ = 13.7 Hz, PNP aryl-C). Anal. For $C_{24}H_{45}NP_2Pt$: Calcd: C, 47.67; H, 7.50; Found: C, 48.23; H, 7.62.

X-ray Structural Analysis of 8. Crystal Data. $C_{24}H_{45}NP_2Pt$, orange chunk, 0.06 × 0.06 × 0.05 mm^3, monoclinic, $P2_{1/c}$, a = 10.996(2) Å, b = 15.479(3) Å, c = 30.094(6) Å, β = 90.71(3)°, from 11184 reflections T = 100(2) K, V = 5121.8(18) Å^3, Z = 8, Fw = 604.64, Dc = 1.568 Mg/m^{-3}, μ = 5.614 mm^{-1}.

Data Collection and Processing. Nonius KappaCCD diffractometer, Mo Kα (λ = 0.71073 Å), graphite monochromator, $0 \le h \le 13$, $0 \le k \le 19$, $-38 \le l \le 38$, frame scan width = 1.0°, scan speed 1.0° per 120 s, typical peak mosaicity 0.365°, 62173 reflections collected, 11278 independent reflections (R_{int} = 0.061). The data were processed with Denzo-Scalepack.

Solution and Refinement. Structure solved by direct methods with SHELXS-97. Full matrix least-squares refinement based on F^2 with SHELXL-97; 531 parameters with no restraints, final R_1 = 0.0312 (based on F^2) for data with $I > 2\sigma(I)$, and R_1 = 0.0452 on 10833 reflections, goodness-of-fit on F^2 = 1.024, largest electron density peak = 1.413 e Å^{-3}. Largest hole −1.118 e Å^{-3}.

Protonation of Complexes 5−8 with Methanol and Water. Complexes **5**−**8** (about 0.01 mmol) were dissolved in a THF solution with a known concentration of methanol or water. Protonation of complexes **5**−**8** with methanol was also carried out in methylene chloride solutions.

Variable Temperature (VT) $^{31}P\{^{1}H\}$ NMR Experiments with Complexes 5−8. A THF solution (0.680 mL) of methanol (107.1 mg, 0.135 mL, 3.347 mmol) and [(PNP*)PdCl] (**5**) (5.5 mg, 0.010 mmol) was placed in an NMR tube. The temperature dependence was followed by $^{31}P\{^{1}H\}$NMR in the range of 293−193 K. In the range of 193−223 K signals of both the cationic and the neutral complexes (complexes **1** and **5**, respectively) were observed. The integration ratios were recorded after reaching equilibrium and $K_{eq}(T)$ (K_{eq} = [**1**]$_{eq}$/[**5**]$_{eq}$[MeOH]$_{eq}$]) was calculated. In a similar experiment a solution of methylene chloride-d_2 was used with methanol-d_4, and the temperature dependence was followed by ^{1}H and $^{31}P\{^{1}H\}$ NMR. However, in methylene chloride only the cationic or the neutral complexes were observed.

Similar experiments were carried out with complex **6** (4.9 mg, 0.008 mmol) in THF (0.609 mL) and methanol (101.4 mg, 0.128 mL, 3.169 mmol) in the range of 193−213 K; complex **7** (5.8 mg, 0.011 mmol) in THF (0.614 mL) and methanol (15.0 mg, 0.019 mL 0.469 mmol) in the range of 193−223 K; and complex **8** (5.7 mg, 0.009 mmol) in THF (0.660 mL) and methanol (14.8 mg, 0.019 mL, 0.463 mmol) at 193K. Uncertainties in thermodynamic quantities were derived from the intercept error of the van't Hoff plot.

[(PNP)PdCl][K] (9).** KN(SiMe$_3$)$_2$ (5 mg, 0.025 mmol) was added to a stirred THF-d_8 solution (0.5 mL) of [(PNP*)PdCl] (12.4 mg, 0.023 mmol) and the color turned to dark brown. The reaction mixture was placed in an NMR tube. Complex **9** is not stable, and upon evaporation it gives complex **5**, probably because of traces of water in the solvent. Addition of MeLi (1.4 M solution in diethylether) in excess (10−20 equiv) to a THF-d8 solution of [(PNP*)PdCl] resulted in the formation of complex **11** after 5 h.

$^{31}P\{^{1}H\}$ NMR (202 MHz, THF-d_8): 55.61 (s). ^{1}H NMR (500 MHz, THF-d_8): 1.55 (vt, 36H, J_{PH} = 6.5 Hz, C(CH_3)$_3$)), 2.69 (vt, 1H, J_{PH} = 3.0 Hz, CH-P), 4.97 (d, 2H, $^{3}J_{HH}$ = 7.8 Hz, PNP-aryl H), 6.1 (m, 1H, PNP-aryl H). $^{13}C\{^{1}H\}$ NMR (126 MHz, THF-d_8): 29.91 (vt, J_{CP} = 3.3 Hz, C(CH_3)$_3$)), 37.32 (vt, J_{CP} = 10.7 Hz, C(CH$_3$)$_3$)), 51.58 (vt, J_{CP} = 25.4 Hz, CH-P), 89.94 (vt, J_{CP} = 9.5 Hz, PNP aryl-CH), 133.32 (s, PNP aryl-CH), 174.92 (vt, J_{CP} = 7.4 Hz, PNP aryl-C).

[(PNP)PtCl][K] (10).** Complex **10** was synthesized in the same manner as complex **9** from [(PNP*)PtCl] (**6**) (14.8 mg, 0.024 mmol) and KN(SiMe$_3$)$_2$ (5.2 mg, 0.026 mmol).

$^{31}P\{^{1}H\}$ NMR (101 MHz, THF-d_8): 46.53 (s, $^{1}J_{PPt}$ = 2577 Hz). ^{1}H NMR (250 MHz, THF-d_8): 1.53 (vt, 36H, J_{PH} = 6.5 Hz, C(CH_3)$_3$), 2.81 (vt, 2H, J_{PH} = 4.2 Hz, $^{3}J_{PtH}$ = 32 Hz, CH-P), 4.92 (d, 2H, $^{3}J_{HH}$ = 7.5 Hz, PNP-aryl H), 5.97 (m, 1H, PNP-aryl H). $^{13}C\{^{1}H\}$ NMR (126 MHz, benzene-d_6): 30.11 (br s, C(CH_3)$_3$), 37.86 (vt, J_{CP} = 14.0 Hz, C(CH$_3$)$_3$), 49.73 (vt, J_{CP} = 31.6 Hz, CH-P), 89.94 (vt, J_{CP} = 9.0 Hz, PNP aryl-CH), 132.38 (s, PNP aryl-CH), 175.83 (vt, J_{CP} = 10.7 Hz, PNP aryl-C).

[(PNP)PdMe][K] (11).** MeLi (1.6 M in ether, 0.58 mmol, 362 μL) was added to a stirred THF-d_8 solution (0.5 mL) of [(PNP*)PdMe] (**7**) (15.0 mg, 0.029 mmol), and the color turned orange. The reaction mixture was placed in an NMR tube. The reaction of complex **7** with 1.1 equiv of KN(SiMe$_3$)$_2$ was found to be sluggish. Alternatively, complex **11** can be prepared by addition of excess MeLi (20 equiv) to a THF solution of [(PNP)PdCl].

$^{31}P\{^{1}H\}$ NMR (162 MHz, THF-d_8): 50.02 (s). ^{1}H NMR (400 MHz, THF-d_8): 0.22 (t, $^{3}J_{PH}$ = 4.0 Hz, Pd-CH_3), 1.20 (vt, 36H, J_{PH} = 6.0 Hz, C(CH_3)$_3$), 4.69 (d, 2H, $^{3}J_{HH}$ = 8.0 Hz, PNP-aryl H), 5.79 (t, 1H, $^{3}J_{HH}$ = 8.0 Hz, PNP-aryl H) (the signal of CH-P is overlapping with the signal of ether). $^{13}C\{^{1}H\}$ NMR (100 MHz, THF-d_8): −21.48 (t, $^{2}J_{CP}$ = 7.7 Hz, Pd-CH_3), 30.41 (vt, J_{CP} = 3.6 Hz, C(CH_3)$_3$), 36.73 (vt, J_{CP} = 9.6 Hz, C(CH$_3$)$_3$), 50.32 (vt, J_{CP} = 25.65 Hz, CH-P), 90.37 (vt, J_{CP} = 8.9 Hz, PNP aryl-CH), 132.93 (vt, J_{CP} = 2.9 Hz, PNP aryl-CH), 173.07 (vt, J_{CP} = 9.0 Hz, PNP aryl-C).

[(PNP)PtMe][K] (12).** Complex **12** was synthesized in the same manner as complex **9** from [(PNP*)PtMe] (**8**) (15.3 mg, 0.025 mmol) and KN(SiMe$_3$)$_2$ (5.4 mg, 0.027 mmol) and gave a red solution.

$^{31}P\{^{1}H\}$ NMR (162 MHz, THF-d_8): 48.77 ($^{1}J_{PPt}$ = 2726 Hz). ^{1}H NMR (400 MHz, THF-d_8): 0.22 (vt, J_{PH} = 4.0 Hz, Pd-CH_3), 1.25 (vt, 36H, J_{PH} = 5.8 Hz, C(CH_3)$_3$), 2.93 (vt, 2H, J_{PH} = 3.7 Hz, $^{3}J_{PtH}$ = 30.7 Hz, CH-P), 4.69 (d, 2H, $^{3}J_{HH}$ = 8.0 Hz, PNP-aryl H), 5.79 (vt, 1H, $^{3}J_{HH}$ = 8.0 Hz, PNP-aryl H).

$^{13}C\{^{1}H\}$ NMR (100 MHz, THF-d_8): −30.78 (t, $^{2}J_{CP}$ = 7.1, $^{1}J_{CPt}$ = 611.2 Hz, Pt-CH_3), 30.30 (vt, J_{CP} = 3.1, $^{3}J_{CPt}$ = 17.8 Hz, C(CH_3)$_3$), 37.56 (vt, J_{CP} = 13.3 Hz, $^{2}J_{CPt}$ = 46.4 Hz, C(CH$_3$)$_3$), 51.38 (vt, J_{CP} = 31.1, $^{2}J_{CPt}$ = 18.1 Hz, CH-P), 89.34 (vt, J_{CP} = 8.4 Hz, PNP aryl-CH), 132.25 (vt, J_{PC} = 2.9 Hz, PNP aryl-CH), 173.96 (vt, J_{PC} = 10.1 Hz, PNP aryl-C).

Acknowledgment. This project was supported by the Israel Science Foundation, by the DIP Program for German−Israeli Cooperation, and by the Helen and Martin Kimmel Center for Molecular Design.

Supporting Information Available: PDF file of X-ray crystallography structures of complexes **2**−**8**, calculated bond lengths (Å) and Wiberg bond indices for **2′**−**4′**, **6′**−**8′**, and **10′**−**12′**, NPA charges of complexes **1′**−**12′** and Cartesian coordinates of all DFT structures. CIF files containing X-ray crystallographic data for complexes **1**−**8**. This material is available free of charge via the Internet at http://pubs.acs.org.